

DTIC FILE COPY

(4)

MEMORANDUM REPORT BRL-MR-3699

**BRL**

1938 - Serving the Army for Fifty Years - 1988

THERMAL DECOMPOSITION OF RDX  
AND RDX-BOROHYDRIDE MIXTURES

MICHAEL A. SCHROEDER

SEPTEMBER 1988

DTIC  
ELECTE  
OCT 1 2 1988  
S H D

APPROVED FOR PUBLIC RELEASE; DISTRIBUTION UNLIMITED.

U.S. ARMY LABORATORY COMMAND

BALLISTIC RESEARCH LABORATORY  
ABERDEEN PROVING GROUND, MARYLAND

88 1011 270

AD-A199 371

**DESTRUCTION NOTICE**

Destroy this report when it is no longer needed. DO NOT return it to the originator.

Additional copies of this report may be obtained from the National Technical Information Service, U.S. Department of Commerce, Springfield, VA 22161.

The findings of this report are not to be construed as an official Department of the Army position, unless so designated by other authorized documents.

The use of trade names or manufacturers' names in this report does not constitute indorsement of any commercial product.

UNCLASSIFIED

SECURITY CLASSIFICATION OF THIS PAGE

REPORT DOCUMENTATION PAGE				Form Approved OMB No. 0704-0188	
1a. REPORT SECURITY CLASSIFICATION Unclassified			1b. RESTRICTIVE MARKINGS		
2a. SECURITY CLASSIFICATION AUTHORITY			3. DISTRIBUTION/AVAILABILITY OF REPORT		
2b. DECLASSIFICATION/DOWNGRADING SCHEDULE					
4. PERFORMING ORGANIZATION REPORT NUMBER(S)			5. MONITORING ORGANIZATION REPORT NUMBER(S)		
6a. NAME OF PERFORMING ORGANIZATION US Army Ballistic Research Laboratory		6b. OFFICE SYMBOL (If applicable) SLCBB-IB	7a. NAME OF MONITORING ORGANIZATION		
6c. ADDRESS (City, State, and ZIP Code) Aberdeen Proving Ground, MD 21005-5066			7b. ADDRESS (City, State, and ZIP Code)		
8a. NAME OF FUNDING/SPONSORING ORGANIZATION		8b. OFFICE SYMBOL (If applicable)	9. PROCUREMENT INSTRUMENT IDENTIFICATION NUMBER		
8c. ADDRESS (City, State, and ZIP Code)			10. SOURCE OF FUNDING NUMBERS		
PROGRAM ELEMENT NO. 61102A		PROJECT NO. AH43	TASK NO.	WORK UNIT ACCESSION NO.	
11. TITLE (Include Security Classification) THERMAL DECOMPOSITION OF RDX AND RDX-BOROHYDRIDE MIXTURES					
12. PERSONAL AUTHOR(S) Michael A. Schroeder					
13a. TYPE OF REPORT Final		13b. TIME COVERED FROM Jan 86 to Dec 86		14. DATE OF REPORT (Year, Month, Day)	
15. PAGE COUNT					
16. SUPPLEMENTARY NOTATION Published in Proceedings, 23rd JANNAF Combustion Meeting					
17. COSATI CODES			18. SUBJECT TERMS (Continue on reverse if necessary and identify by block number)		
FIELD 07	GROUP 03	SUB-GROUP	RDX, Nitramines, Borohydrides, Boron Hydrides, Catalysis		
07	04		Mechanisms, Catalysis, Propellants, Explosives, Thermal		
			Decomposition, Gun Propellants, VHBR Propellants, Combustion		
19. ABSTRACT (Continue on reverse if necessary and identify by block number) This report is a progress report on GCMS studies on the thermal decomposition of RDX, both alone and in mixtures with $K_2B_{12}H_{12}$ . This work differs from previous work in that the less-volatile decomposition products are emphasized, rather than the gaseous products such as $N_2O$ , $H_2C=O$ , and $NO$ . A number of these less-volatile products are formed. 1,3,5-triazine has been conclusively identified for the first time as a decomposition product of RDX. This is mechanistically significant because it suggests the operation of either some form of $N-NO_2$ cleavage or of intermolecular CH abstraction. Crude estimates of the effects on 1,3,5-triazine formation of temperature and of added $K_2B_{12}H_{12}$ have been made and are briefly discussed. Other products are still under study; those identified to date include mononitroso-RDX (MRDX) and unreacted RDX.					
20. DISTRIBUTION/AVAILABILITY OF ABSTRACT <input type="checkbox"/> UNCLASSIFIED/UNLIMITED <input checked="" type="checkbox"/> SAME AS RPT. <input type="checkbox"/> DTIC USERS			21. ABSTRACT SECURITY CLASSIFICATION Unclassified		
22a. NAME OF RESPONSIBLE INDIVIDUAL DR. MICHAEL A. SCHROEDER			22b. TELEPHONE (Include Area Code) 301-278-6105		22c. OFFICE SYMBOL SLCBB-IB-I

DD Form 1473, JUN 86

Previous editions are obsolete.

SECURITY CLASSIFICATION OF THIS PAGE

UNCLASSIFIED

# TABLE OF CONTENTS

	<u>Page</u>
LIST OF FIGURES.....	5
LIST OF TABLES .....	7
I. INTRODUCTION.....	9
II. EXPERIMENTAL.....	9
III. RESULTS.....	10
IV. DISCUSSION.....	29
A. Identification of Chromatographic Peaks.....	29
B. Preliminary Observations Concerning Catalyst and Temperature Effects on Formation of 1,3,5-Triazine.....	30
C. Chemical Mechanisms.....	32
ACKNOWLEDGEMENTS.....	38
REFERENCES.....	39
DISTRIBUTION LIST.....	41



Accession For	
NTIS GRA&I	<input checked="" type="checkbox"/>
DTIC TAB	<input type="checkbox"/>
Unannounced	<input type="checkbox"/>
Justification	
By	
Distribution	
Availability Codes	
Avail and/or	
Dist	Special
A-1	

# LIST OF FIGURES

<u>Figure</u>		<u>Page</u>
1	Total Ion Chromatogram from RDX Decomposed 20 sec at 250°C.....	11
2	Total Ion Chromatogram from RDX + K <sub>2</sub> B <sub>12</sub> H <sub>12</sub> Decomposed 20 sec at 250°C.....	11
3	Total Ion Chromatogram from RDX Decomposed 20 sec at 400°C.....	11
4	Total Ion Chromatogram from RDX + K <sub>2</sub> B <sub>12</sub> H <sub>12</sub> Decomposed 20 sec at 400°C.....	11
5	Total Ion Chromatogram from RDX Decomposed 20 sec at 600°C.....	12
6	Total Ion Chromatogram from RDX + K <sub>2</sub> B <sub>12</sub> H <sub>12</sub> Decomposed 20 sec at 600°C.....	12
7	Total Ion Chromatogram from RDX Decomposed at 800°C.....	12
8	Total Ion Chromatogram from RDX + K <sub>2</sub> B <sub>12</sub> H <sub>12</sub> Decomposed 20 sec at 800°C.....	12
9a	Mass Spectrum of Peak from RDX Decomposed 20 sec at 800°C.....	13
9b	NBS Library Spectrum of 1,3,5-Triazine.....	13
9c	Mass Spectrum of Authentic Sample of 1,3,5-Triazine, Run on the HP 5890-5970 MSD Used in the Present Work.....	13
10	Mass Spectrum of Chromatographic Peak with Highest m/e = 70.....	14
11a	Typical Mass Spectrum of Chromatographic Peak at ca 1.7 Minute, RDX Alone Decomposed at 250°C.....	14
11b	Same, RDX-K <sub>2</sub> B <sub>12</sub> H <sub>12</sub> Decomposed at 250°C.....	14
12	Typical Mass Spectrum of Chromatographic Peak at ca 2.1 Minutes....	15
13	Typical Mass Spectra for Chromatographic Peak at ca 3.0 Minutes....	15
14	Typical Mass Spectrum of Chromatographic Peak Beleived to be 1,3,5-Triazine N-Oxide.....	16
15	Typical Mass Spectrum of Chromatographic Peak at ca 4.6 Minutes....	16
16	Typical Mass Spectrum of Chromatographic Peak at ca 4.9 Minutes....	17
17	Typical Mass Spectrum of Chromatographic Peak at ca 7.5 Minutes....	17
18	Typical Mass Spectrum of Chromatographic Peak at ca 8.2 Minutes....	18
19	Typical Mass Spectrum of Chromatographic Peak at ca 8.6 Minutes....	18

# LIST OF FIGURES (CONT'D)

<u>Figure</u>		<u>Page</u>
20	Typical Mass Spectrum of Chromatographic Peak at ca 9.2 Minutes....	19
21	Typical Mass Spectrum of Chromatographic Peak at ca 9.4 Minutes....	19
22	Typical Mass Spectrum of Chromatographic Peak at ca 9.9 Minutes....	20
23	Typical Mass Spectrum of Chromatographic Peak at ca 10.5 Minutes...	20
24	Typical Total Ion Chromatogram From $K_2B_{12}H_{12}$ "Decomposed" 20 sec at 600°C.....	21
25	Typical Mass Spectrum of Chromatographic Peak at ca 0.4 Minutes from "Decomposition" of $K_2B_{12}H_{12}$ 20 sec at 800°C.....	21

# LIST OF TABLES

<u>Table</u>		<u>Page</u>
1	Areas and Area Ratios of Some Mass-Spectral Peaks in the Poorly-Retained Products, Pyroprobe at 250°C for 20 Seconds.....	22
2	Areas and Area Ratios of Some Mass-Spectral Peaks in the Poorly-Retained Products, Pyroprobe at 400°C for 20 Seconds.....	23
3	Areas and Area Ratios of Some Mass-Spectral Peaks in the Poorly-Retained Products, Pyroprobe at 600°C for 20 Seconds.....	24
4	Areas and Area Ratios of Some Mass-Spectral Peaks in the Poorly-Retained Products, Pyroprobe at 800°C for 20 Seconds.....	25
5	Effect of Alternating Catalyzed and Uncatalyzed Runs on Areas and Area Ratios of Some Mass-Spectral Peaks in the Poorly-Retained Products.....	26
6	Table of Peaks in Total Ion Chromatograms from RDX and RDX-K <sub>2</sub> B <sub>12</sub> H <sub>12</sub> Decompositions.....	27

## I. INTRODUCTION

Very high burning rate (VHBR) propellants are needed for such applications as the monolithic charge and the traveling charge. These propellants generally contain RDX (hexahydro-1,3,5-trinitro-1,3,5-triazine) and/or triaminoguanidine nitrate (TAGN) together with a borohydride such as one of the HIVELITES (Teledyne-McCormick-Selph). The borohydride greatly accelerates the burning rate of the propellant. The purpose of the present work is to elucidate the chemical mechanisms responsible for the burning rate acceleration, with the ultimate goal of optimizing propellant formulations for demonstration of the traveling charge concept, e.g., maximum "catalytic" effects with minimum sensitivity.

The approach employed involves gas chromatographic-mass spectroscopic (GC-MS) studies on the pyrolysis products of pure RDX and of RDX- $K_2B_{12}H_{12}$  mixtures. A number of previous studies (reviewed in References 2-7) have reported detailed analysis of the permanent gaseous products from decomposition of HMX (octahydro-1,3,5,7-tetranitro-1,3,5,7-tetrazocine) and for RDX. The present work is concentrated mainly on the less-volatile products, namely those whose volatilities are intermediate between those of the more-commonly-studied permanently gaseous products on the one hand, and that of unreacted RDX on the other.

## II. EXPERIMENTAL

RDX was obtained by crystallization of Class A military grade RDX from acetone. This reduced the HMX content from ca 5-10% to ca 0.3%. In an attempt to minimize particle-size effects, a portion of RDX was ground in a mortar for several minutes and divided into two portions, one of which was mixed with the  $K_2B_{12}H_{12}$  and the other used in the uncatalyzed runs. Use of a set of standard selves showed that the average particle size was about 100 $\mu$ . A sample of  $K_2B_{12}H_{12}$  was obtained from Callery Chemical Company, Callery, Pennsylvania. The GC-MS experiments were carried out using a Hewlett-Packard (HP) 5890 gas chromatograph, with a HP 5970 mass-selective detector and a 59970B workstation consisting of a 9133 disk drive, 9100-236 computer and associated software (including library search software and complete NBS library of about 38,000 compounds), printer and plotter. The software is capable of producing complete spectra at any point, as well as either total ion chromatograms (plots of total-ion intensity vs. time), or ion chromatograms (plots of intensity vs. time for any particular ion or group of ions). Pyrolyses were carried out with a Chemical Data Systems (CDS) "Pyroprobe" pyrolyzer with coil probe, which was fitted to the injection port of the 5890 gas chromatograph by means of a heated interface, which was also obtained from CDS. The pyrolysis temperatures given are pyroprobe set temperatures.

In a typical run, an unweighed sample (ca 1 milligram) was put into a quartz tube 25 mm long having an inside diameter of 2 mm; the sample was retained in the tube with small plugs of quartz wool on either side. The sample was pyrolyzed by heating the probe to the desired temperature (given in the tables) with the fastest possible heating rate (ca 75°C/msec) and holding it there for 20 seconds. A split inlet was employed, with a split ratio of ca 30. The GC carrier gas was helium, with a flow rate through the column of ca 0.5 ml/min. Total flow was ca 40-45 ml/min, and the inlet purge flow was



ca 6 ml/min. The GC column was an HP-1 column (crosslinked methyl silicone gum, 12 m long, 0.2 mm i.d.; 0.3  $\mu$ m film thickness); the initial GC oven temperature was 70°C, for 3 minutes followed by heating at 20°C/minute to a final temperature of 210°C, followed by a final 5-minute hold time.

### III. RESULTS

Chromatograms and mass spectra were obtained for decomposition of RDX alone, and for an RDX- $K_2B_{12}H_{12}$  mixture containing 19%  $K_2B_{12}H_{12}$ . Several runs were carried out at each of the following temperatures: 250, 400, 600 and 800°C. Typical chromatograms are shown in Figures 1-8.

Tables 1-4 include a summary of intensities of some of the more significant peaks in the spectra of 1,3,5-triazine formed in the decompositions. These tables represent series of runs carried out on the same day, all runs on a given day being carried out either with or without added  $K_2B_{12}H_{12}$ . An additional series of runs was carried out (Table 5), in which runs with and without added  $K_2B_{12}H_{12}$  were alternated on the same day; it was hoped that this alternation of catalyzed and uncatalyzed runs on the same day would minimize differences between runs due to factors such as operator technique. The numbers in Tables 1-5 represent integrated total-ion intensities in the region 0-1 minute (Column 4), and integrated intensities of the single-ion intensities of the peaks at ca 0.5 minute in the single-ion chromatograms for m/e 44, 54, and 81. These were by far the most intense peaks in the chromatograms.

Figures 9a-9c are respectively the spectrum of a typical 1,3,5-triazine peak from the present work; the NBS library spectrum of 1,3,5-triazine; and the mass spectrum of an authentic sample of 1,3,5-triazine obtained on our apparatus.

Table 6 is a table of retention times for the most important peaks observed in the chromatograms of the products of the decomposition runs. The numbers in the "Figure" column of this table are those of the figures in the present report which give typical spectra for the respective peaks; these spectra are given in Figures 10-23. Note that many of the spectra in Figures 9-25 undoubtedly represent mixtures rather than pure components. This can be seen from some of the entries in Table 6, as well as from the baseline elevation in the 0.5-14 minute region of Figures 1-8.

Figure 24 is a chromatogram from heat-treatment of  $K_2B_{12}H_{12}$  at 600°C; note that it contains two peaks, one at ca 0.4 minutes and the other at ca 6 minutes. Peak intensities increased with increasing temperature, as did the intensity of the second peak relative to the first. The 0.6 minute peak was identified from its mass spectrum as triethylamine, presumably remaining in traces from preparation of the  $K_2B_{12}H_{12}$ . The 0.4 minute peak remains unidentified. A typical mass spectrum of the 0.4 minute peak is shown in Figure 25; this spectrum resulted from decomposition at 800°C.

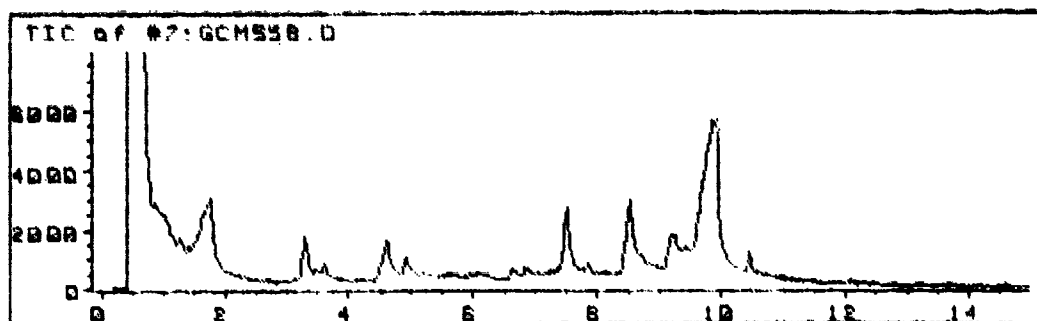


Figure 1. Total Ion Chromatogram from RDX Decomposed 20 sec at 250°C

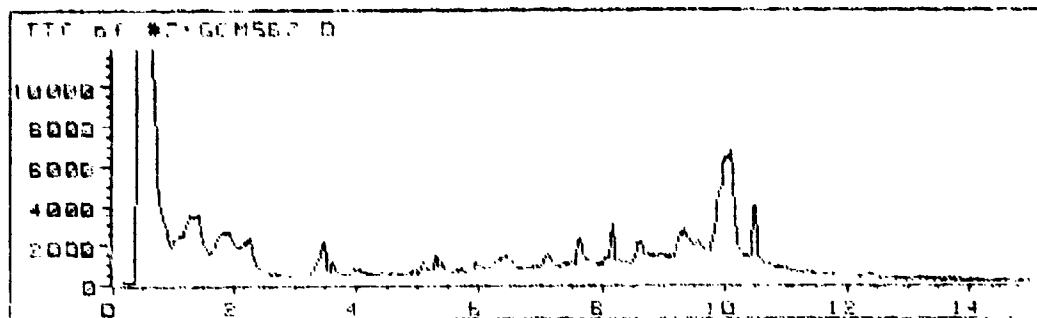


Figure 2. Total Ion Chromatogram from RDX +  $K_2B_{12}H_{12}$  Decomposed 20 sec at 250°C

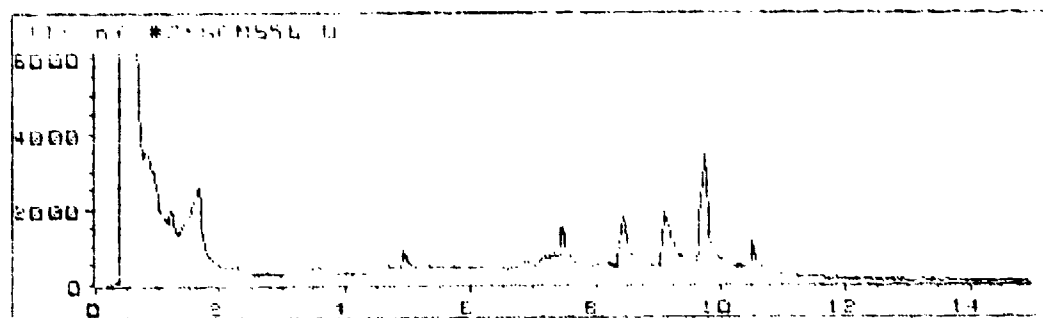


Figure 3. Total Ion Chromatogram from RDX Decomposed 20 sec at 400°C

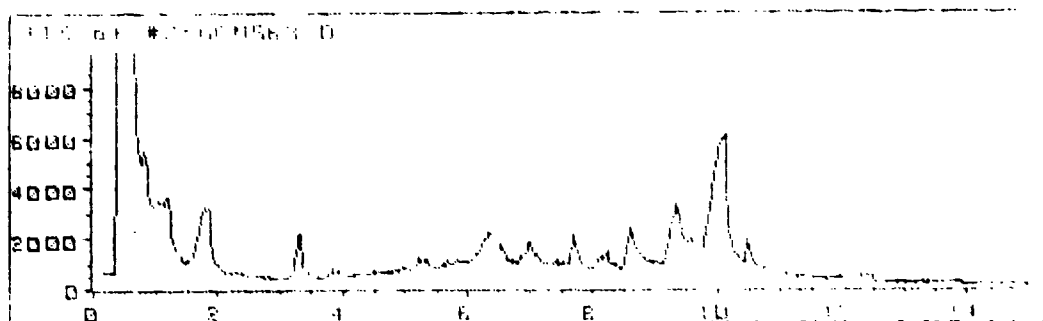


Figure 4. Total Ion Chromatogram from RDX +  $K_2B_{12}H_{12}$  Decomposed 20 sec at 400°C



Figure 5. Total Ion Chromatogram from RDX Decomposed 20 sec at 600°C

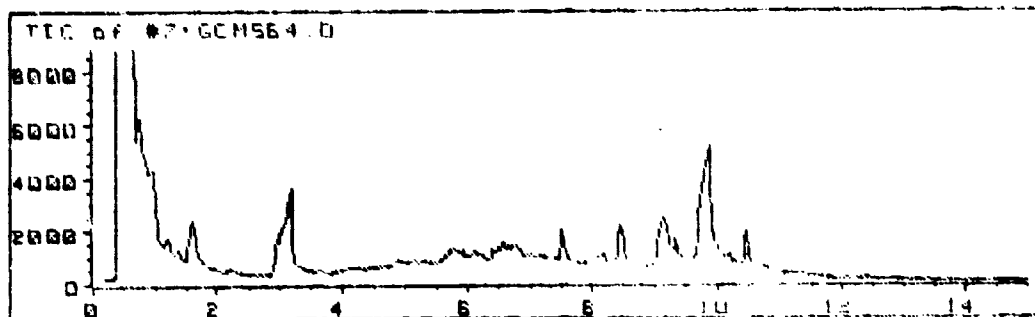


Figure 6. Total Ion Chromatogram from RDX +  $K_2B_{12}H_{12}$  Decomposed 20 sec at 600°C

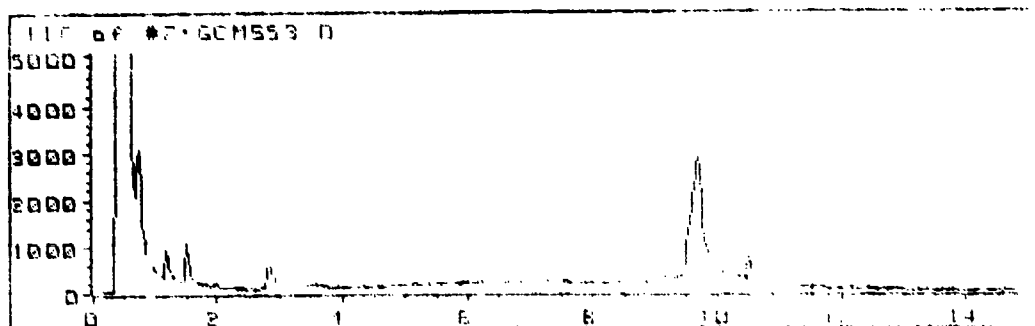


Figure 7. Total Ion Chromatogram from RDX Decomposed at 800°C

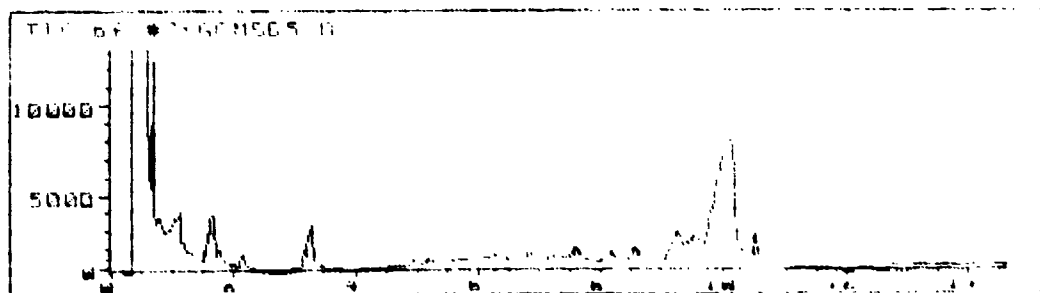


Figure 8. Total Ion Chromatogram from RDX +  $K_2B_{12}H_{12}$  Decomposed 20 sec at 800°C

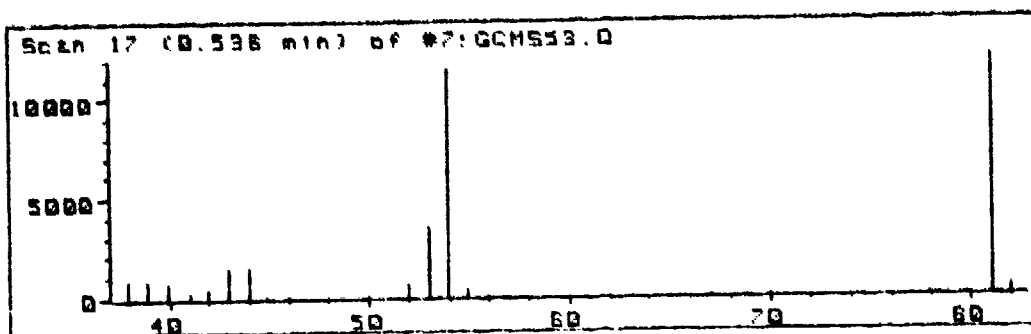


Figure 9a. Mass Spectrum of Peak from RDX Decomposed 20 sec at 800°C

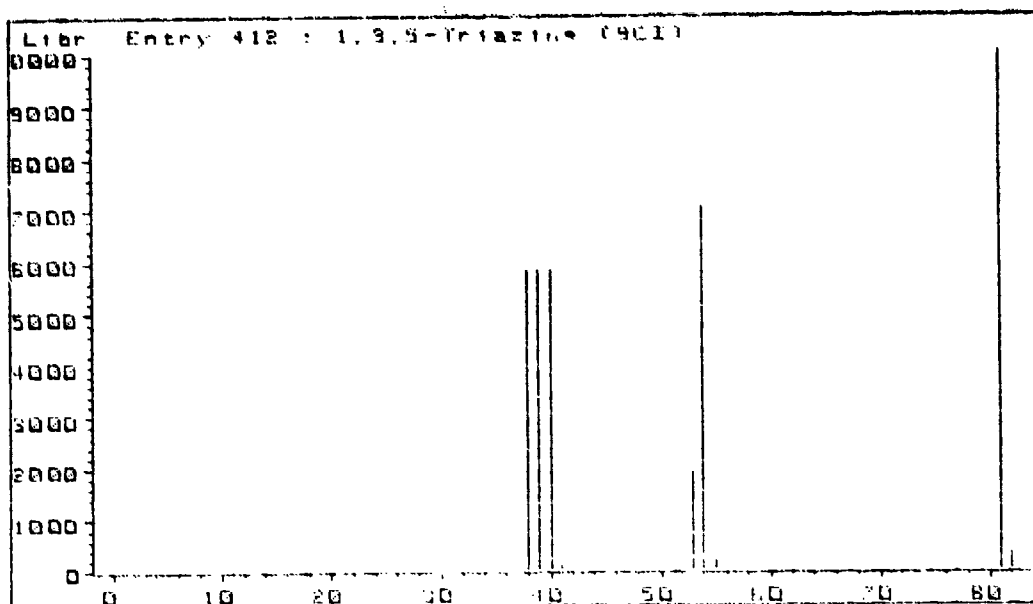


Figure 9b. NBS Library Spectrum of 1,3,5-Triazine

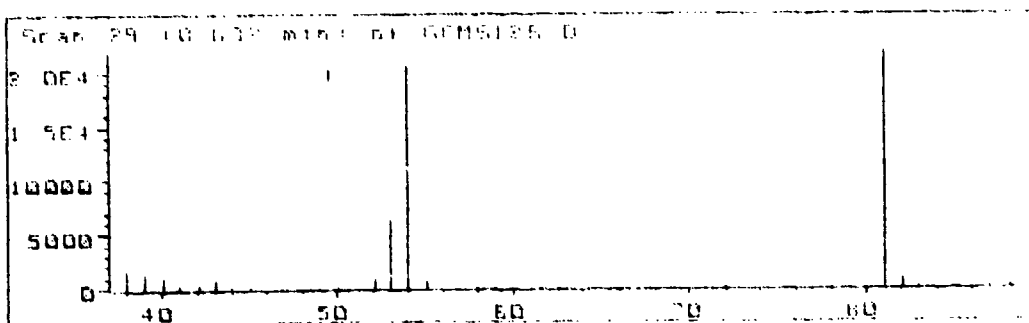


Figure 9c. Mass Spectrum of Authentic Sample of 1,3,5-Triazine, Run on the HP 5890-5970 MSD Used in the Present Work

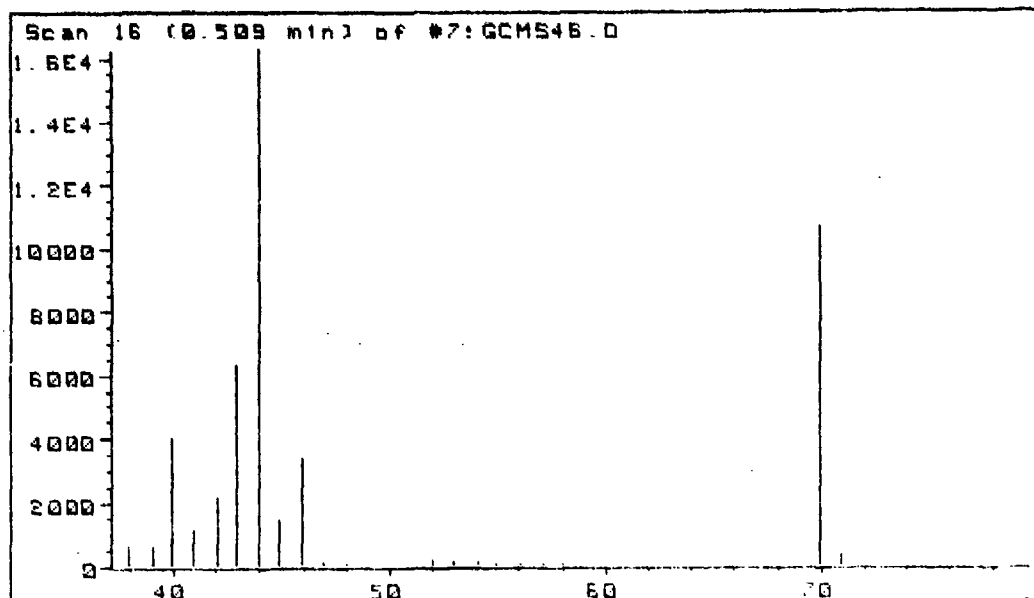


Figure 10. Mass Spectrum of Chromatographic Peak with Highest  $m/e = 70$ . The lines at  $m/e$  44 and 46 are due to overlapping gaseous-product peaks.

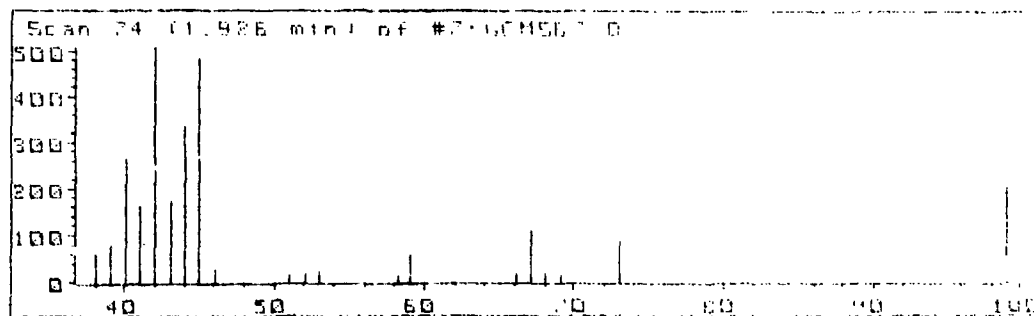
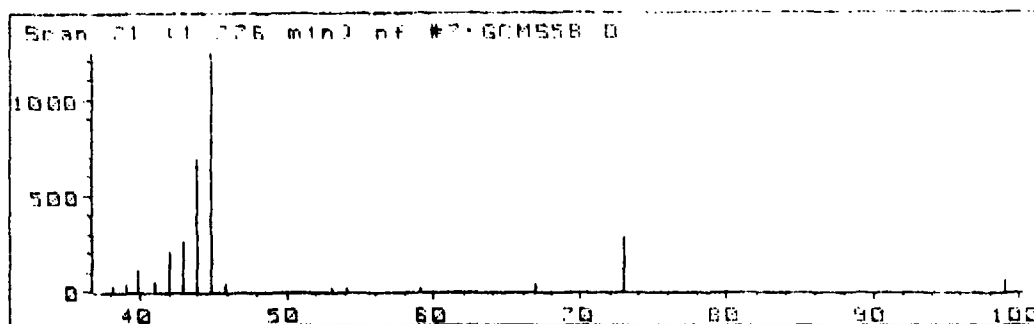


Figure 11. a. Typical Mass Spectrum of Chromatographic Peak at ca 1.7 Minute, RDX Alone Decomposed at 250°C. b. Same, RDX- $K_2B_{12}H_{12}$  Decomposed at 250°C.

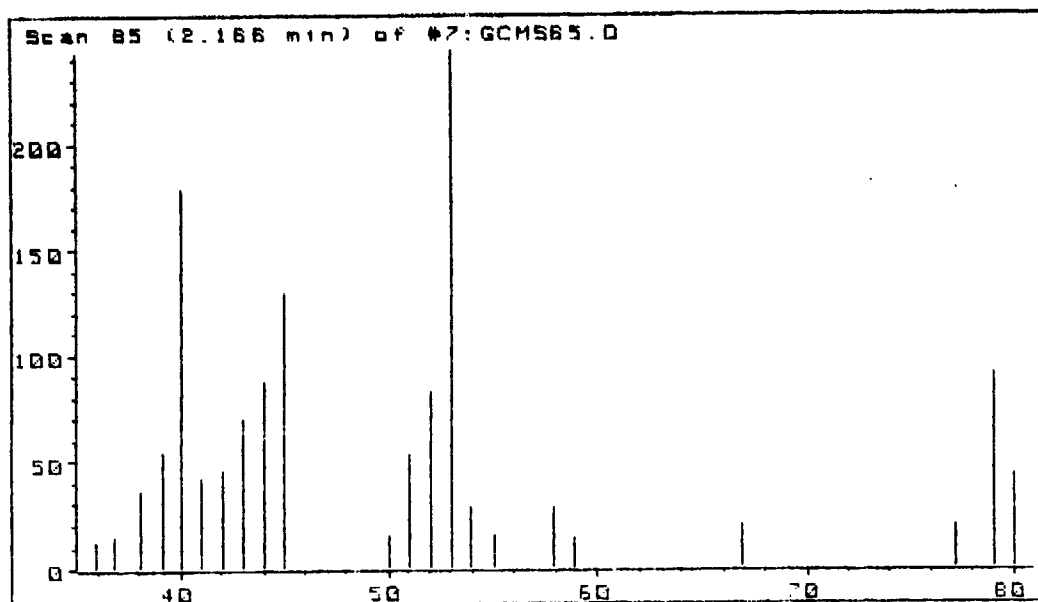


Figure 12. Typical Mass Spectrum of Chromatographic Peak at ca 2.1 Minutes

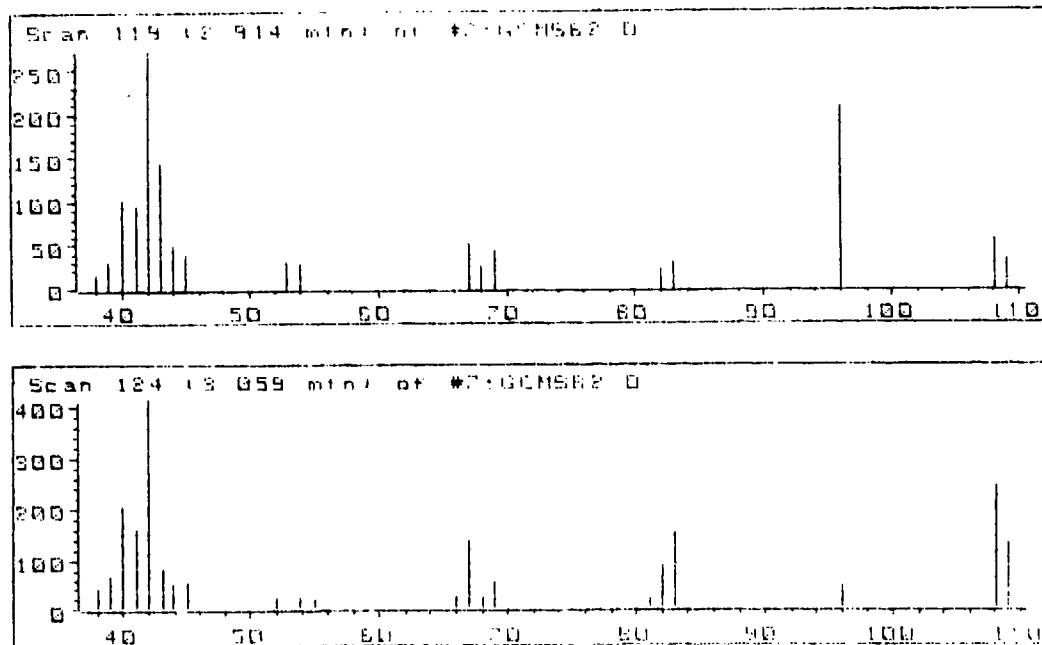


Figure 13. Typical Mass Spectra for Chromatographic Peak at ca 3.0 Minutes

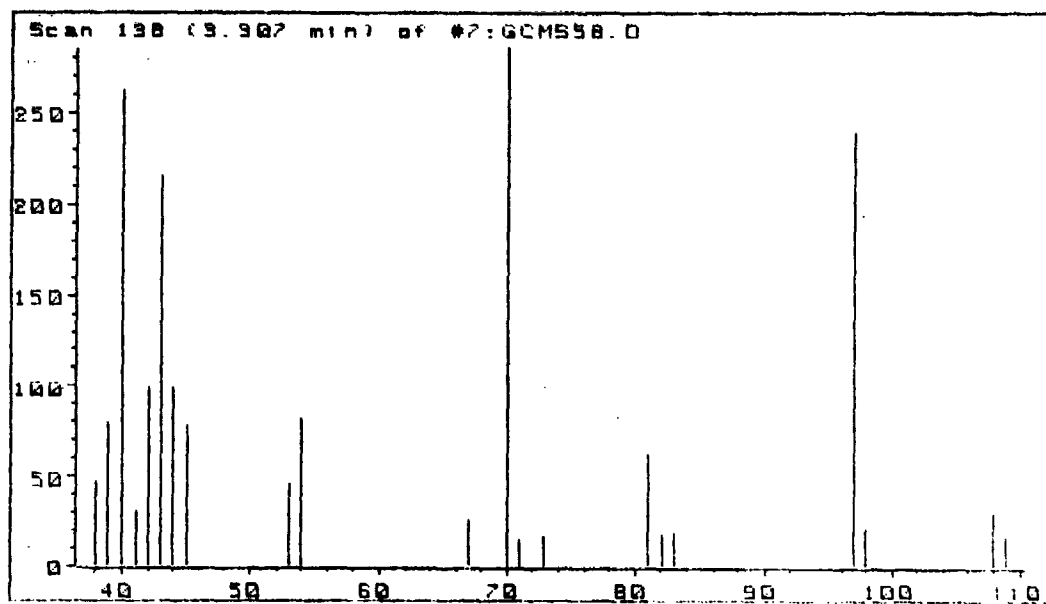


Figure 14. Typical Mass Spectrum of Chromatographic Peak Beleived to be 1,3,5-Triazine N-Oxide

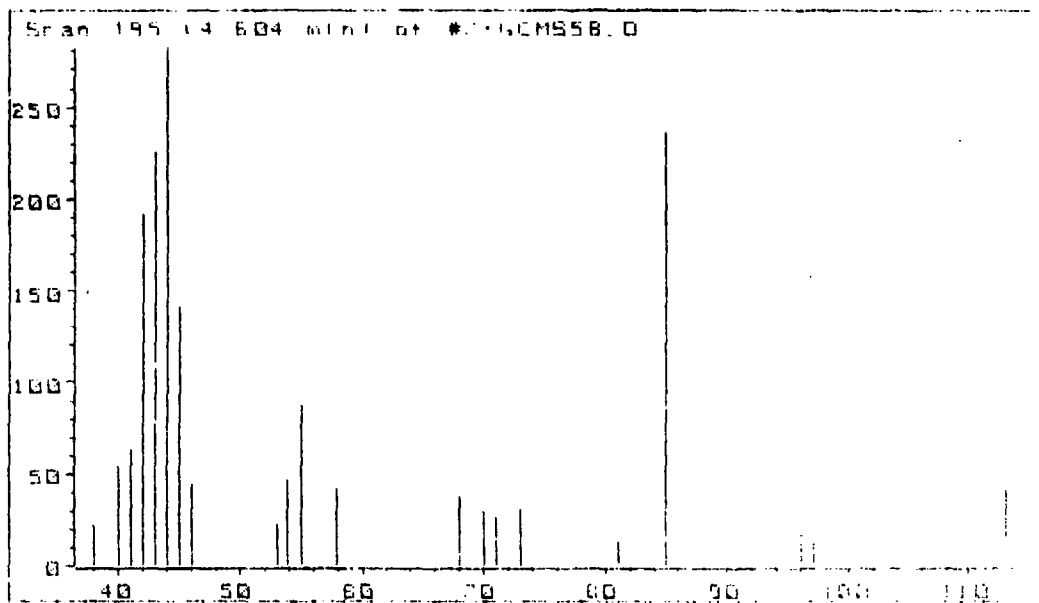


Figure 15. Typical Mass Spectrum of Chromatographic Peak at ca 4.6 Minutes

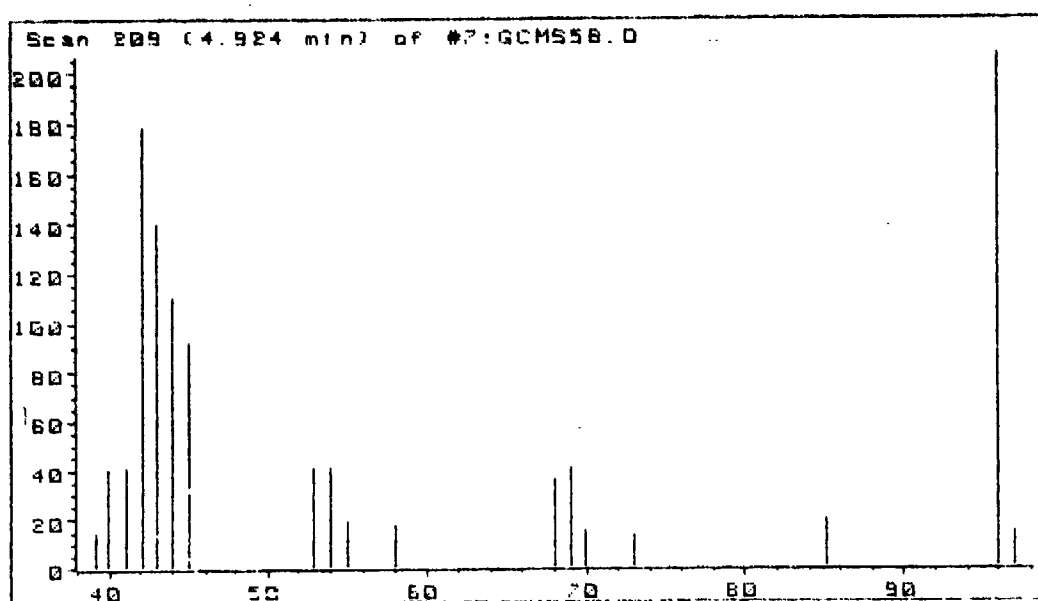


Figure 16. Typical Mass Spectrum of Chromatographic Peak at ca 4.9 Minutes

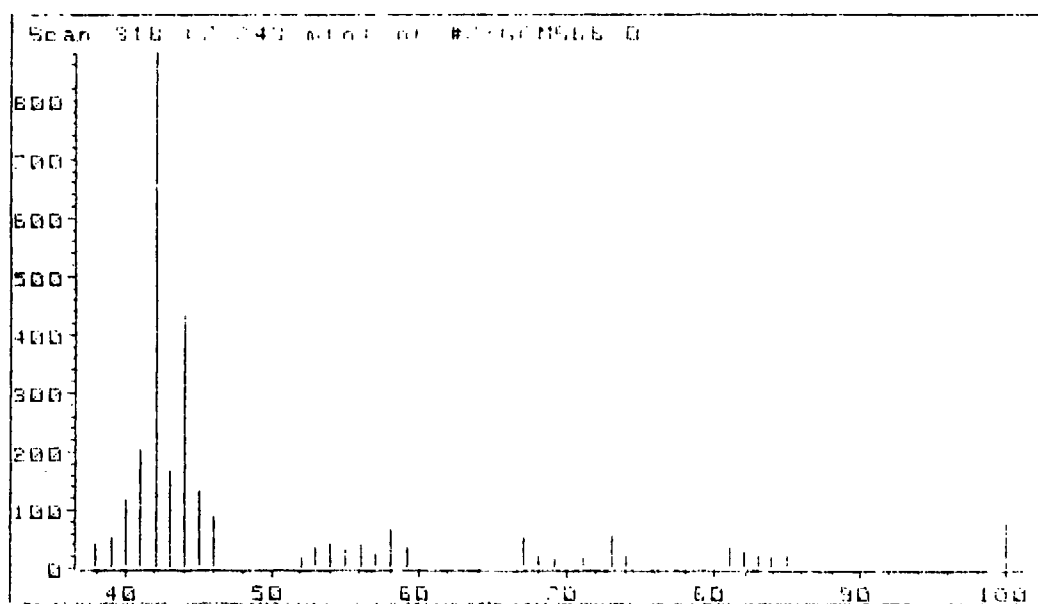


Figure 17. Typical Mass Spectrum of Chromatographic Peak at ca 7.5 Minutes



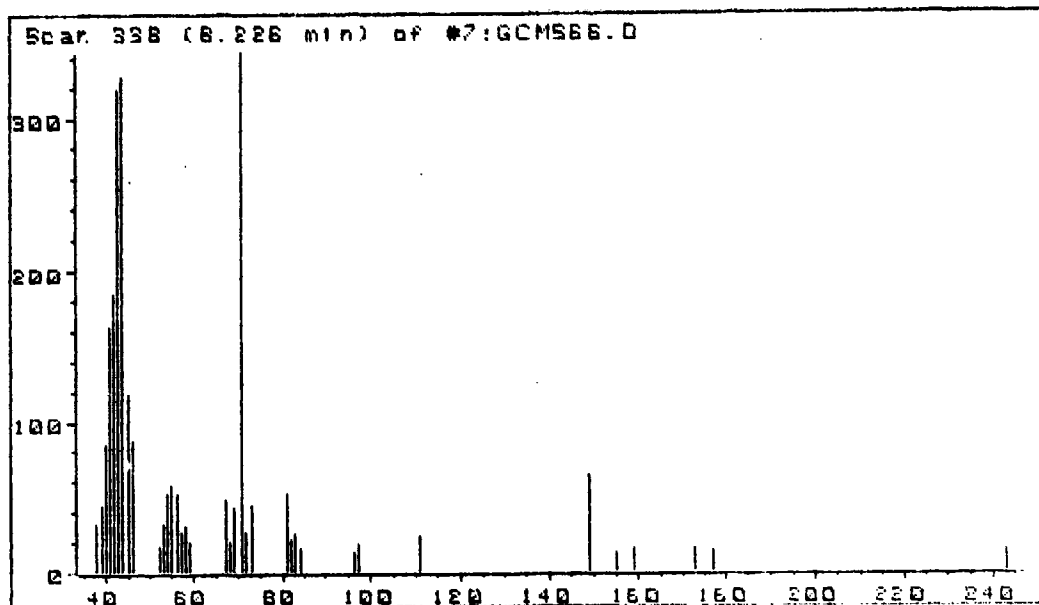


Figure 18. Typical Mass Spectrum of Chromatographic Peak at ca 8.2 Minutes

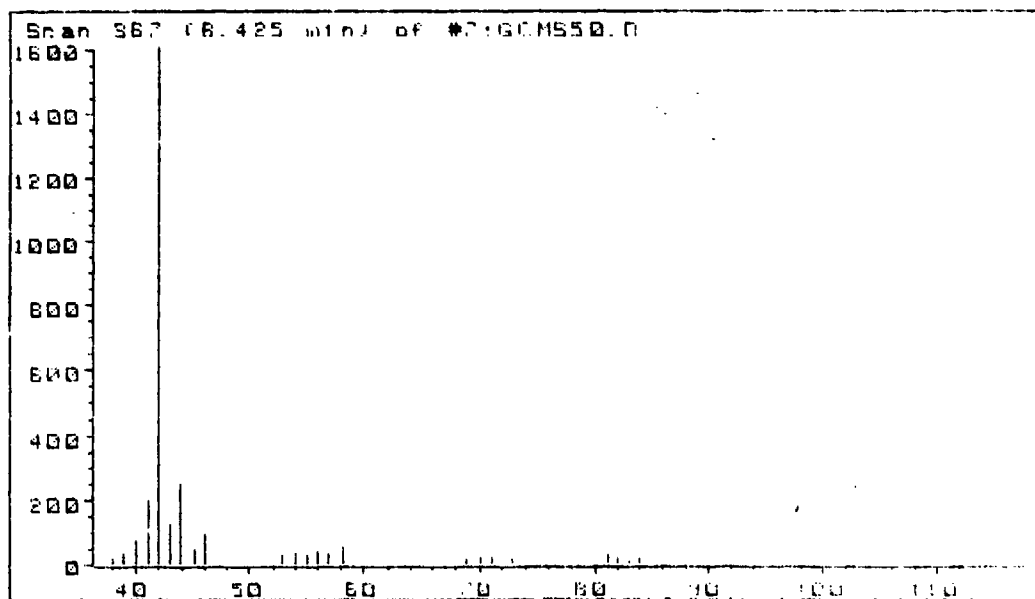


Figure 19. Typical Mass Spectrum of Chromatographic Peak at ca 8.6 Minutes

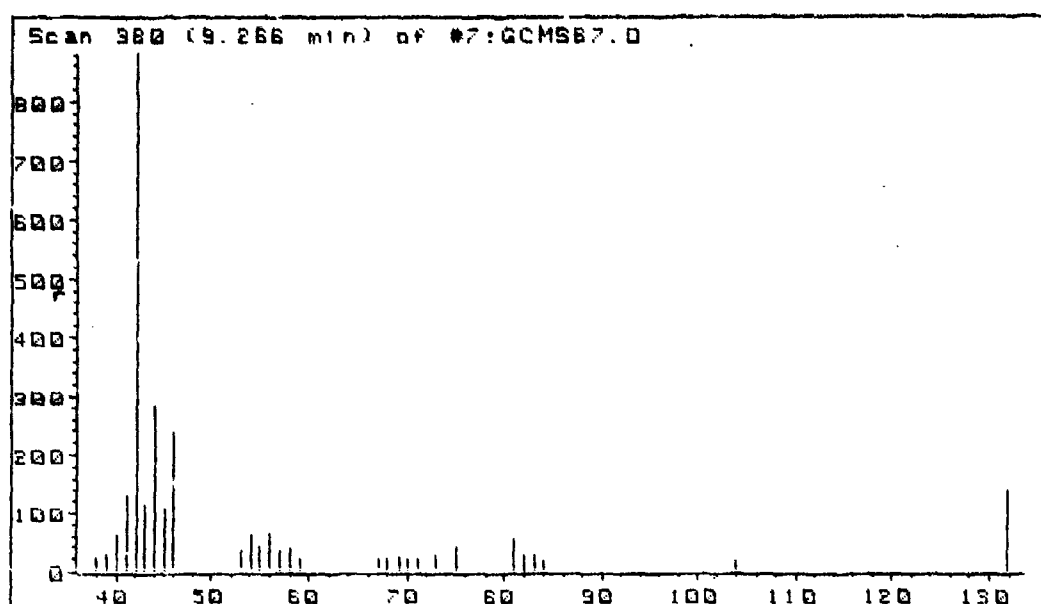


Figure 20. Typical Mass Spectrum of Chromatographic Peak at ca 9.2 Minutes

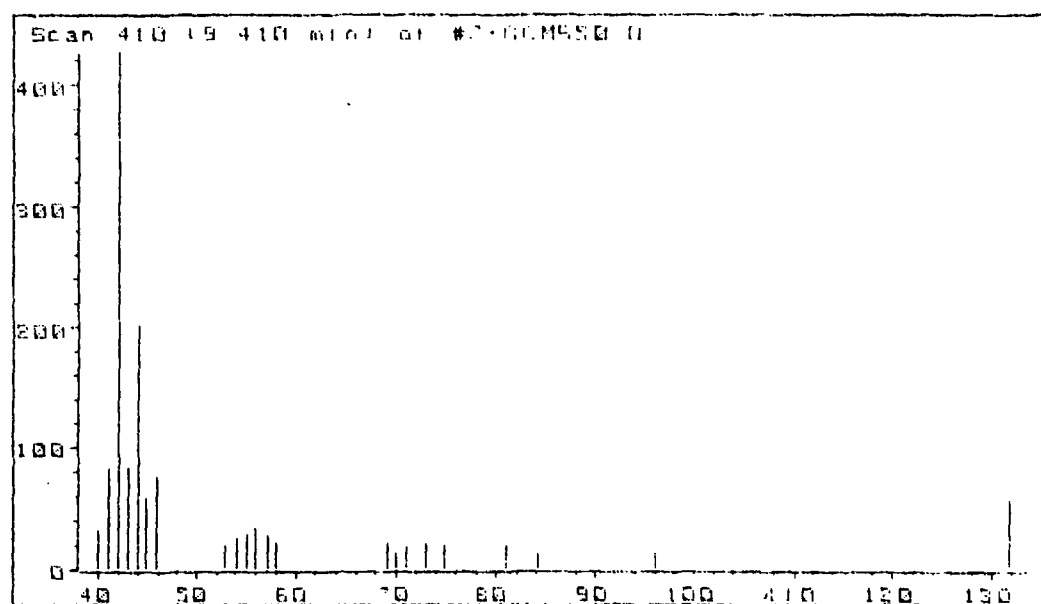


Figure 21. Typical Mass Spectrum of Chromatographic Peak at ca 9.4 Minutes

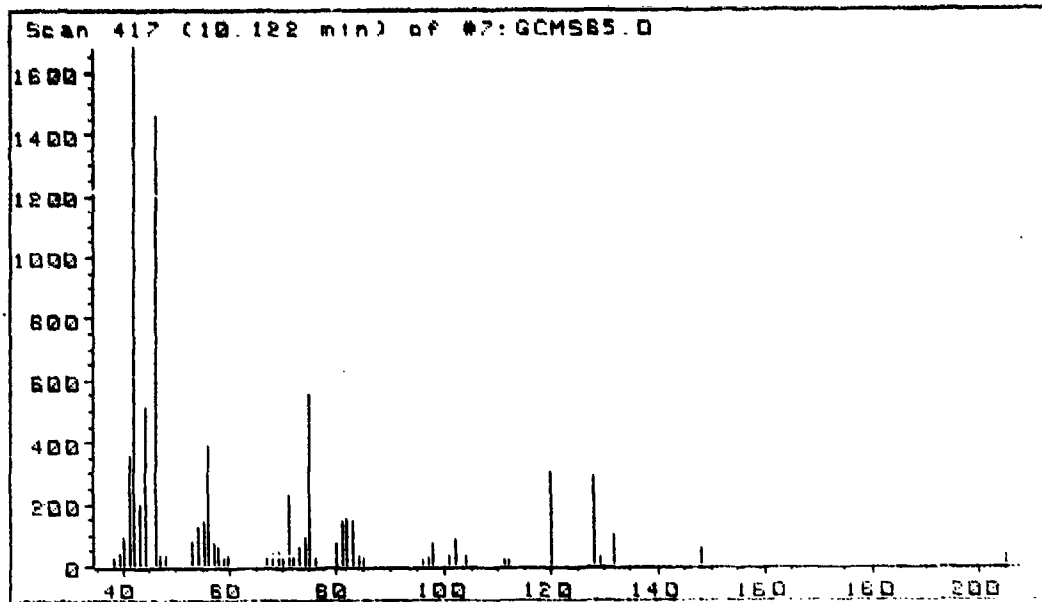


Figure 22. Typical Mass Spectrum of Chromatographic Peak at ca 9.9 Minutes

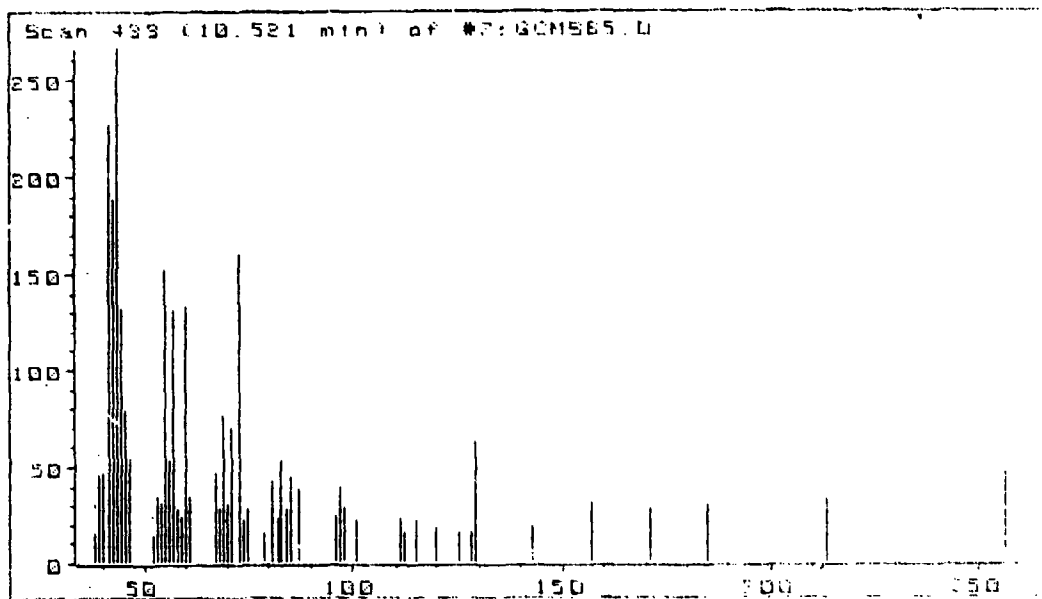


Figure 23. Typical Mass Spectrum of Chromatographic Peak at ca 10.5 Minutes

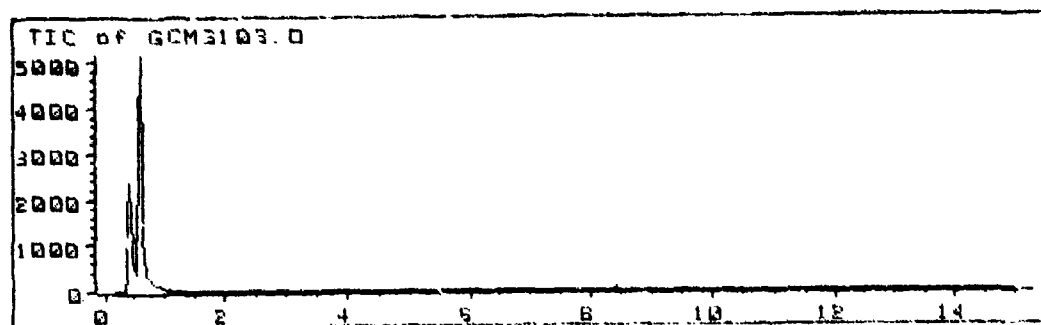


Figure 24. Typical Ion Chromatogram From  $K_2B_{12}H_{12}$  "Decomposed" 20 sec at 600°C

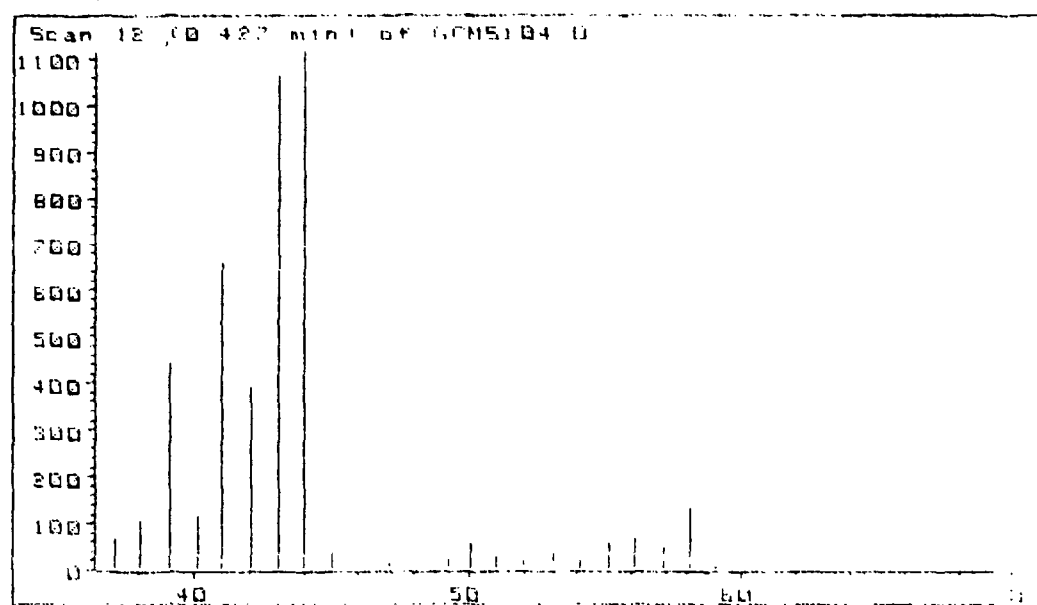


Figure 25. Typical Mass Spectrum of Chromatographic Peak at ca 0.4 Minutes from "Decomposition" of  $K_2B_{12}H_{12}$  20 sec at 800°C

Table 1. Areas and Area Ratios of Some Mass-Spectral Peaks in the Poorly-Retained Products,  
Pyroprobe at 250°C for 20 Seconds

Run	Date	Cat.?	Peak Areas ( $\times 10^6$ ) at m/e				Area Ratios		
			Tot	44	54	81	44/Tot	54/Tot	81/Tot
46a	6/24/86	No	5.34*	2.85	0.161*	0.193*	0.534	0.0301*	0.0361*
50a	6/25/86	No	4.95*	2.89	0.357	0.404	0.584	0.0721	0.0816
58a	6/27/86	No	4.90*	2.56	0.341	0.389	0.522	0.0696	0.0794
72b	7/9/86	No	42.30	5.03	0.297*	0.338*	0.119	0.00702*	0.00799*
60a	7/1/86	Yes	5.98*	3.71	0.456	0.524	0.620	0.0763	0.0876
61a	7/1/86	Yes	4.49*	3.04	0.242	0.282	0.677	0.0539	0.0628
67a	7/2/86	Yes	6.58*	4.05*	0.345*	0.398*	0.615	0.0524*	0.0605*
74b	7/15/86	Yes	5.25*?	0.763	0.0658	0.0736	0.145	0.0125	0.0140
78b	7/15/86	Yes	11.56	1.753	0.0960*?	0.103*?	0.152	0.00830*?	0.00891*?
									0.0548*?
									0.0588*?

a - Masses 35-400 scanned

b - Masses 3-400 scanned

\* - Complex (Two or more clear peaks)

\*? - Slight Complexity (Shoulder or small second peak)

Table 2. Areas and Area Ratios of Some Mass-Spectral Peaks in the Poorly-Retained Products,  
Pyroprobe at 400°C for 20 Seconds

Run	Date	Cat.?	Peak Areas (x10 <sup>6</sup> ) at m/e			44/Tot	Area Ratios		
			Tot	44	54		81/Tot	54/44	81/44
49a	6/24/86	No	5.25*	2.74	0.168*	0.194*	0.032*	0.0370*	0.0613*
51a	6/25/86	No	4.45*	2.25	0.214*	0.251*	0.0481*	0.0564*	0.0951*
55a	6/26/86	No	5.72*	2.57	0.321*	0.372*	0.0561*	0.0650*	0.120*
56a	6/27/86	No	4.83*	2.44	0.427	0.487	0.0884	0.101	0.175
71b	7/9/86	No	34.6	3.24\$	0.700*?	0.793*?	0.0202*?	0.0231*?	0.216*?
63a	7/1/86	Yes	5.81*	3.70\$?	0.326*	0.363*	0.0561*	0.0625*	0.0881*
66a	7/2/86	Yes	1.82*	4.77\$	0.405*	0.474*	0.0518*	0.0606*	0.0949*
75b	7/15/86	Yes	11.65	1.21	0.0642*	0.0721*	0.00549*	0.00619*	0.0531*

a - Masses 35-400 scanned

b - Masses 3-400 scanned

\* - Complex (Two or more clear peaks)

\*? - Slight Complexity (Shoulder or small second peak)

\$ - Slightly flat-topped peak

Table 3. Areas and Area Ratios of Some Mass-Spectral Peaks in the Poorly-Retained Products, Pyroprobe at 600°C for 20 Seconds

Run	Date	Cat.?	Peak Areas (x10 <sup>6</sup> ) at m/e	81	44/Tot	54/Tot	Area Ratios	
			Tot				81/Tot	54/44
52a	6/25/86	No	4.56*	1.95	0.484	0.529	0.428	0.106
57a	6/27/86	No	6.58*	2.62	0.767	0.826	0.398	0.117
70b	7/9/86	No	59.71	4.20	1.31	1.46	0.0703	0.0219
64a	7/2/86	Yes	6.72*	3.60	0.665	0.759	0.536	0.0990
68a	7/2/86	Yes	7.91*	3.89	0.731	0.828	0.492	0.0924
76b	7/15/86	Yes	14.56*	1.33	0.127*?	0.135*?	0.0913	0.00872*?
							0.00927*?	0.0954*?
								0.102*?

a - Masses 35-400 scanned

b - Masses 3-400 scanned

\* - Complex (Two or more clear peaks)

?? - Slight Complexity (Shoulder or small second peak)

Table 4. Areas and Area Ratios of Some Mass-Spectral Peaks in the Poorly-Retained Products,  
Pyroprobe at 800°C for 20 Seconds

Run	Date	Cat.?	Peak Areas ( $\times 10^6$ ) at m/e				Area Ratios		
			Tot	44	54	81	44/Tot	54/Tot	81/Tot
53a	6/25/86	No	4.045*	1.90	0.391	0.430	0.470	0.0967	0.107
54a	6/26/86	No	5.07*	2.34	0.429	0.483	0.462	0.0846	0.0953
59a	6/27/86	No	3.69*	2.09	0.150	0.177	0.566	0.0406	0.0480
69b	7/9/86	No	44.46	4.31	0.646	0.722	0.0969	0.0145	0.0162
73b	7/9/86	No	50.00	4.90	0.704	0.784	0.0980	0.0141	0.0157
62a	7/1/86	Yes	5.34*	3.11	0.383	0.417	0.582	0.0717	0.0781
65a	7/2/86	Yes	6.76*	3.78	0.525	0.587	0.559	0.0777	0.0868
77b	7/15/86	Yes	16.11*?	1.29\$?	0.124	0.134	0.0801	0.00770	0.00832
									0.0961
									0.104

a - Masses 35-400 scanned

b - Masses 3-400 scanned

\* - Complex (Two or more clear peaks)

\*? - Slight Complexity (Shoulder or small second peak)

\$ - Slightly flat-topped peak



Table 5. Effect of Alternating Catalyzed and Uncatalyzed Runs on Areas and Area Ratios of Some Mass-Spectral Peaks in the Poorly-Retained Products

Run	Date	Cat.?	Temp	Peak Areas ( $\times 10^6$ ) at m/e			Area Ratios		
				Tot	44	54	54/Tot	81/Tot	54/44
31a	5/16/86	Yes	600	1.25*	1.02	Present	0.816	0.084	0.10
32a	5/16/86	No	600	8.08*	4.59	0.68	0.568	0.10	0.15
33a	5/16/86	Yes	600	6.04*	4.50	0.20	0.745	0.043	0.044
34a	5/16/86	No	600	2.25*	1.24	0.169	0.551	0.089	0.136
35a	5/20/86	Yes	600	12.92	7.79	0.71	0.603	0.055	0.091
36a,b	5/20/86	No	600	11.80	7.26	0.755	0.621	0.064	0.104
43a	6/19/86	Yes	600	5.66*	2.42	0.49	0.428	0.0866	0.0919
44a	6/19/86	No	600	4.36*	1.65	0.44	0.378	0.101	0.112
45a	6/19/86	Yes	600	5.33	2.44	0.48*?	0.458	0.090*?	0.197*?
23a,c	5/13/86	Yes	250	8.08*	4.76	0.207*	0.589	0.026*	0.043*
25a,d	5/13/86	No	250	9.15*	5.44	0.225*	0.594	0.025*	0.041*
27a,e	5/14/86	Yes	250	11.30*	7.24	0.247*	0.641	0.022*	0.034*
29a,c	5/14/86	No	250	6.83*	3.65	0.319*	0.534	0.047*	0.087*

a - Masses 35-400 scanned

b - Atypical run - helium leak caused broad peaks and long retention times

c - Fresh tube

d - Tube used for run 23, probably contaminated with  $K_{12}B_{12}H_{12}$  residue, therefore not a typical uncatalyzed run

e - Tube used for runs 23-25

\* - Complex (Two or more clear peaks)

\*? - Slight Complexity (Shoulder or small second peak)

Table 6. Table of Peaks in Total Ion Chromatograms from RDX and  
RDX-K<sub>2</sub>B<sub>12</sub>H<sub>12</sub> Decompositions

Time (minutes)	Occurrence	Spectrum (Figure)	Remarks
ca 0-1	All Conditions	9a (Triazine) 10 (Oxadiazole(?))	Includes permanent gases (N <sub>2</sub> O, CO <sub>2</sub> ), 1,3,5-triazine and a peak with highest mass at m/e 70 (1,2,4- oxadiazole?)
ca 1-2.5	All Conditions	1-8*	Especially at low temperatures, this region is difficult to characterize. It sometimes includes broad, variable peaks whose spectra resemble formamide.
1.7±0.2	All Conditions	11	Appears under all conditions. Looks like a mixture. A: Highest mass = 99. B: Highest mass = 73. Is R HC(=O)NHC(=O)H or Dimethylformamide?
2.1	High-T Cat.	12	Sometimes present at high temperature, from decomposition with added K <sub>2</sub> B <sub>12</sub> H <sub>12</sub> .
3.0±0.4	All Conditions	13	Spectrum shows this is not 1,3,5-triazine N-oxide. Present under all conditions, especially at high temperature with added K <sub>2</sub> B <sub>12</sub> H <sub>12</sub> . Looks like a mixture. A: Highest mass = 108/109. B: Highest mass = 96.
3.3	Low-T Uncat.	14	1,3,5-Triazine N-oxide (tentative). Sometimes appears at low (250°C) temperature for RDX alone; not seen at higher temperatures or with added K <sub>2</sub> B <sub>12</sub> H <sub>12</sub> .
4.6	Low-T Uncat.	15	From decomposition at low (250, 400 C) temperature, without added K <sub>2</sub> B <sub>12</sub> H <sub>12</sub> .

Table 6. Table of Peaks in Total Ion Chromatograms from RDX and  
RDX-K<sub>2</sub>B<sub>12</sub>H<sub>12</sub> Decompositions (CONT'D)

Time (minutes)	Occurrence	Spectrum (Figure)	Remarks
4.9	Low-T Uncat.	16	From some decomposition runs at low (250, 400°C) temperature, without added K <sub>2</sub> B <sub>12</sub> H <sub>12</sub> .
ca 5-7	All	1-8*	This region included a number of weak peaks, especially from decomposition at low (250, 400°C) temperature, with added K <sub>2</sub> B <sub>12</sub> H <sub>12</sub> . A peak with m/e 58 is sometimes seen at ca 6.5 min; is this hydroxymethylformamide - OH?
7.6±0.1	Catalyzed; Low-T Uncat.	17	Not reproducible. Usually highest m/e = 100, sometimes 110, 114, 149 or 177. Not seen for RDX alone at high temperature.
8.2	Catalyzed	18	Sometimes occurs, especially in presence of K <sub>2</sub> B <sub>12</sub> H <sub>12</sub> . Does this contain B <sub>4</sub> fragments?
8.6±0.1	Catalyzed; Low-T Uncat.	19	Not seen for RDX alone at high temperature.
9.2±0.2	All Conditions	20	Occurs under most conditions, even weakly at high (800°C) temperature. Has m/e 132; beleived to be MRDX.
9.4±0.1	All Conditions	21	Occurs under most conditions, even weakly at high (800°C) temperature. Has m/e 132; is this DRDX?
9.9±0.2	All Conditions	22	Unreacted RDX; always present regardless of temperature or presence of K <sub>2</sub> B <sub>12</sub> H <sub>12</sub> .
10.5	All Conditions	23	Often present regardless of temperature or presence of borohydride.

\*Total Ion Chromatogram.

#### IV. DISCUSSION

##### A. Identification of Chromatographic Peaks

Figures 1-8 show total ion chromatograms for typical catalyzed and uncatalyzed runs carried out at 250, 400, 600 and 800°C. The more important chromatographic peaks are tabulated in Table 6 and their spectra are shown in Figures 10-23. Even under similar conditions of temperature and presence/absence of catalyst, some variations in presence and intensity of certain peaks were seen. However these chromatograms are typical of those obtained under the conditions in question. Identification of the various peaks in these complex systems is still in progress, and at present many peaks remain unidentified. Some complete and partial identifications are discussed below. Some apparent patterns in effect of catalysis and temperature on the relative degree of formation of 1,3,5-triazine, one of the more mechanistically significant products formed, are then discussed briefly.

Note that, in these chromatograms, the relatively very intense peak(s) at the beginning of the chromatogram (retention time ca one-half minute) correspond to the gaseous products<sup>1-5</sup> ( $N_2O$ , formaldehyde, CO,  $CO_2$ ,  $N_2$ , etc.), that are examined in most studies<sup>1-7</sup> on HMX and RDX decomposition, while the weaker peaks following it are due to less-volatile products, with retention strengths approximately intermediate between those of the permanent gaseous products and unreacted RDX.

Unreacted RDX. Other than the gaseous-product peak at ca 0.5 minute, the most intense peak in the chromatograms shown in Figures 1-8 occurs at ca 9.8-10 minutes. This peak is identified as unreacted RDX by comparison of its mass spectrum with a reference spectrum contained in the NBS library (Table 6, Figure 22).

1-Mononitroso-3,5-dinitro-hexahydro-1,3,5-triazine (mononitroso-RDX, MRDX). The peak at ca  $9.15 \pm 0.2$  minutes (Table 6, Figure 20) is tentatively identified as MRDX, based on comparison of its mass spectra and retention times with those obtained by injection of an acetone solution of an authentic sample of a mixture of MRDX and DRDX; the author thanks Professor T.R. Brill for furnishing this sample. The question of the presence of dinitroso-RDX (DRDX) and trinitroso-RDX among the decomposition products is still under investigation. Nitrosoamines have been detected previously in HMX and RDX decomposition,<sup>4-6,8,9,10</sup> especially in the liquid phase and in solution.

Formamide,  $HC(=O)NH_2$ . A number of the decomposition runs gave spectra closely resembling that of formamide for a peak in the 0.8-1.3 minute region. Non-pyrolytic injections of an authentic sample of formamide suggest that its retention time on the column used is in this region, and can be quite broad. However this identification should be considered uncertain due to the spread in retention times and the observation of extra (impurity?) ion-fragments in the mass spectra of the peaks in question.

1,3,5-Triazine. A number of runs gave computer-run NBS library searches in which one of the best matches for a peak at ca 0.6 minutes was 1,3,5-triazine; see for example Figure 9a. The three peaks at m/e 38, 39, and 40 are weaker in our spectrum (Figure 9a) than in the NBS spectrum (Figure 9b). This possible source of uncertainty was resolved by injecting an authentic

sample of 1,3,5-triazine into our apparatus (Figure 9b); this also showed weaker peaks at  $m/e$  38, 39, and 40. Thus it seems reasonable to conclude that the above intensity difference is due to variations between our 5970 MSD and the spectrometer that was used to record the authentic spectrum contained in the NBS library and reproduced in Figure 9c. Even though not all runs showed a separate peak at this point on their respective total-ion chromatograms, all did have selected ion chromatograms showing reasonably strong peaks at ca 0.6 min for  $m/e$  81 (parent peak of 1,3,5-triazine) and  $m/e$  54 (parent-HCN). It therefore seems reasonable to conclude that under these conditions, 1,3,5-triazine is formed in every run. Furthermore, peak shapes for the peaks at  $m/e$  54 and 81 were identical within a given run; this suggests that these ion-chromatogram peaks came through the column in the same compound.

Peaks in the mass spectra of decomposing RDX and HMX have previously been attributed<sup>12,13</sup> to 1,3,5-triazine and closely related species. Also, 1,3,5-triazine has been detected from its multiphoton dissociation of RDX in a molecular beam.<sup>14a</sup> However, the present work is apparently the first report of its separation and identification by chromatographic techniques.

Additional Compounds Possibly Present. Several additional compounds are at least suggested by the mass spectra of various chromatographic peaks, but without authentic samples or at least spectra on hand, it is hard to be sure. These compounds include dimethylformamide,  $HC(=O)-N(CH_3)_2$ ; oxadiazole derivative (five-membered cyclopentadieneoid ring containing two nitrogens and one oxygen); and 1,3,5-triazine N-oxide.

The 1,3,5-triazine oxide peak was seen in the absence of  $K_2B_{12}H_{12}$  at 250°C, but was greatly reduced or eliminated at higher temperatures and in the presence of  $K_2B_{12}H_{12}$ . Note also that detection of 1,3,5-triazine oxide would be in agreement with detection of peaks at  $m/e$  97 and 98 in atmospheric pressure chemical ionization studies<sup>11</sup> on RDX decomposition which have been carried out at CRDEC.

The peaks of almost equal intensity at  $m/e$  43 and 44 in the 8.2 minute peak (Figure 18) and in the 0.4 minute peak from  $K_2B_{12}H_{12}$  at 800°C (Figure 25) seem at least consistent with the presence of  $B_4$  fragments.<sup>14b</sup>

#### B. Preliminary Observations Concerning Catalyst and Temperature Effects on Formation of 1,3,5-Triazine

Columns 4-7 of Tables I-IV contain summaries of integrated total intensities of the almost-unretained (retention time less than ca 0.8 minute) products, as well as of the peaks corresponding to  $m/e$  44 (believed to be mostly  $CO_2$  and  $N_2O$ ), 54 and 81 (the two strongest peaks in the mass spectrum of 1,3,5-triazine, see Figure 9.). The last five columns of Tables 1-4 contain the ratios of the areas of the peaks  $m/e$  44, 54 and 81 to the total ion area, and of the integrated areas of the  $m/e$  54 and 81 ions to the  $m/e$  44 ion. The purpose of the ratioing was to compensate at least partially for the fact that the samples were unweighed, thereby obtaining at least a crude normalized estimate of the relative amounts of 1,3,5-triazine formed in the various runs. This seemed worthwhile because of the possible mechanistic significance of the formation of 1,3,5-triazine. Note however the possibility

of uncertainty due to such factors as changes with temperature or degree of catalysis in the relative amounts of the gaseous products.

General Considerations. The portion (ca 0-0.8 minute) of the total ion chromatogram corresponding to the almost-unretained products often showed several peak maxima, apparently due to the presence of several different products. These runs are indicated by an asterisk adjacent to the number in column 4 (Tables 1-4) or 5 (Table 5).

Furthermore, the peaks at ca 0.6 minute in the ion chromatograms for m/e 54 and 81 (strongest peaks in the mass spectrum of 1,3,5-triazine) were often complex, exhibiting a shoulder or even two distinct peaks. Peaks exhibiting this behavior are indicated by an asterisk next to the numbers in columns 6 and 7 (Tables 1-4) or 7 and 8 (Table 5). This complexity occurred most often in the runs carried out at the two lowest temperatures (250 and 400°C.), and often appeared to parallel reduced yields of 1,3,5-triazine (m/e 54 and 81) relative to total products and m/e 44. The reasons for this behavior are not understood. Possible explanations include: (a) Vaporization of some RDX out of the quartz tube, followed by condensation on the walls of the interface in which the pyroprobe is inserted and/or the ends of the tube, and further decomposition of the condensate, resulting in two spurts of gaseous decomposition products. This seems unlikely, however, since the interface was maintained at 150°C, a temperature at which decomposition should be too slow to give a second spurt of decomposition products only a few seconds behind the first. A second possibility might be (b) sequential formation of 1,3,5-triazine by two different decomposition mechanisms, resulting in two spurts of 1,3,5-triazine; however there is no evidence for this. A third possibility involves (c) decomposition of different portions of the sample at different times, due to uneven distribution of the sample in the tube. This does not seem unreasonable, in view of the length of the pyrolysis event (20 seconds or even more, since there was undecomposed material remaining in the tube after the 250 degree decompositions), compared to the time (several seconds) between the two portions of the split peak. The reduced amounts of 1,3,5-triazine formed in runs with complex m/e 54 and 81 peaks could possibly be explained in terms of (a) or (c) if the triazine is formed at least partially in a bimolecular reaction of unreacted RDX with a decomposition product, since such reactions might be expected to be less important if the sample is small or highly dispersed.

The m/e 54 and 81 peaks marked with asterisks in the tables were not considered in preparing the following discussion, since it was felt that they might not be comparable with the runs whose m/e 54 and 81 peaks were relatively well-behaved. In a few cases, asterisked peaks whose complexity seemed only slight are marked with a question mark next to the asterisk; these peaks were considered but given less weight.

The m/e 44 peaks seem fairly well-behaved; in only a very few cases are there any complexities or odd-shaped peaks. Furthermore, the area ratios between these peaks and the total ion intensities show much less variation for a given temperature and degree of catalysis than do the m/e 54 and 81 peaks. This indicates that the mass spectrometer and associated computers and integrating software are functioning properly, and that the apparent unruly behavior of the 1,3,5-triazine peaks at m/e 54 and 81 is not due to instrument malfunction or to operator error.

Effect of Catalyst on Relative Intensities of m/e 44 and 1,3,5-Triazine Peaks. If the asterisked m/e 54 and 81 peaks are dropped from consideration, it appears (Tables 1-5) that addition of  $K_2B_{12}H_{12}$  as a catalyst causes (a) an increase in relative amount of m/e 44 ( $N_2O$  and  $CO_2$ ), and (b) a decrease in relative amount of 1,3,5-triazine formed. These conclusions follow from the last five columns of the tables, which show area ratios for the m/e 54 and 81 peaks to the total intensity and to the intensity of the m/e 44 peak, and for the m/e 44 peak to the total intensity. There are some exceptions, for example run 59 (Table 4) is an exception to both correlations and run 77, also in Table 4, is an exception to (a). The amount of change caused by adding the  $K_2B_{12}H_{12}$  also seems to vary from run to run, being for example negligible in run 60 but significant in run 61 (Table 1). Nevertheless, based on the preponderance of the data in Tables 1-5, it seems reasonable to draw conclusions (a) and (b).

Effect of Temperature on Relative Intensities of m/e 44 and 1,3,5-Triazine Peaks. Increasing the decomposition temperature between 250°C and 600°C causes a decrease in the relative amount of m/e 44 and an increase in the relative amount of the 1,3,5-triazine peaks (m/e 54 and 81); but these trends are not continued on increasing temperature further, to 800°C. In the 250-600 degree range this is in agreement with previous work<sup>4,6,7</sup> which suggests that the amount of products such as  $N_2O$ ,  $N_2$  and  $H_2CO$  decreases with increasing decomposition temperature, while the yields of products such as HCN, NO and  $NO_2$  increase. Possible explanations for failure of the trends to continue to the 800°C region include temperature-induced shifts<sup>4</sup> in the composition and/or amount of decomposition products, or thermal decomposition of 1,3,5-triazine at temperatures above 600°C.

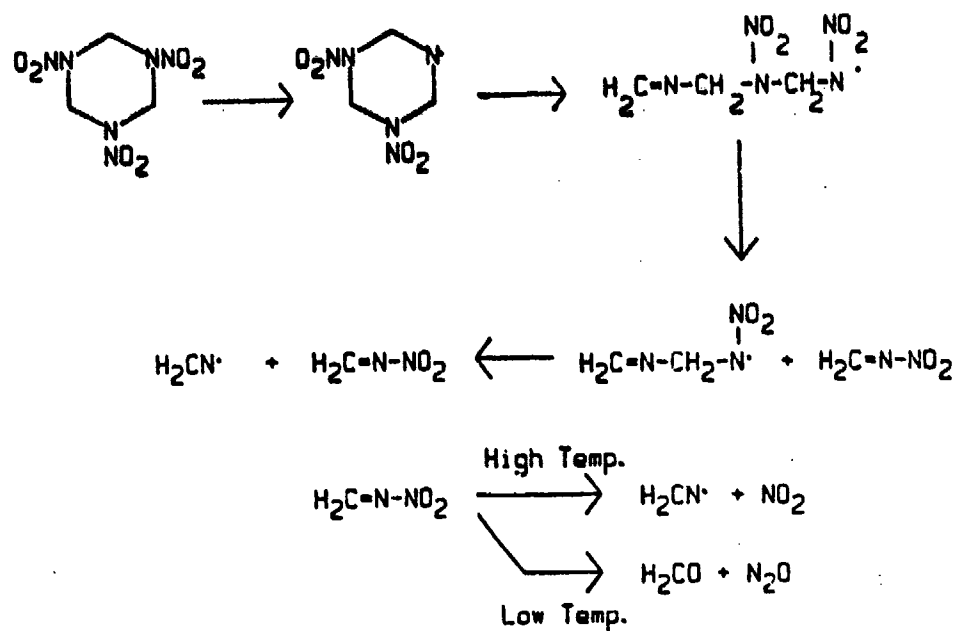
### C. Chemical Mechanisms

Chemical Mechanisms Involved in the Uncatalyzed Decomposition of HMX and RDX. The ultimate goal of the present work involves reaching an understanding of the chemical mechanisms involved in borohydride catalysis of nitramine decomposition. However in order to accomplish this it will of course be necessary to understand the decomposition of uncatalyzed HMX and RDX as a baseline on which to base our understanding of the borohydride-catalyzed decomposition of these materials.

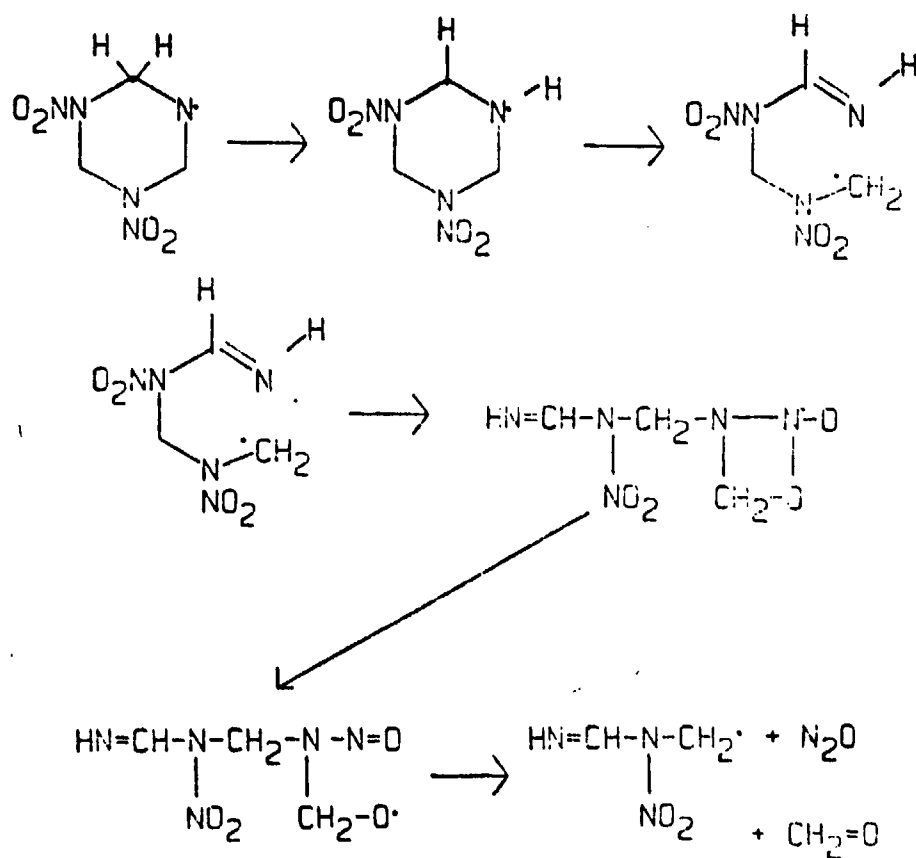
Note that the following discussion refers specifically to thermal decomposition and not to the ion fragmentation seen in mass spectrometers. The present writer generally thinks of RDX decomposition in the liquid phase as proceeding through a main pathway involving chemical mechanisms similar to the following (References 1-7; see especially References 4-6).

There is an observed tendency for formation of more HCN and  $NO_2$  and less  $H_2C=O$  and  $N_2O$  at higher temperatures and heating rates; this could possibly be understood<sup>6</sup> in terms of a shift between the pathways shown (Scheme I) for decomposition of  $H_2C-N-NO_2$ . Note that intermediacy of the N-nitroformimine  $H_2C=N-NO_2$  is not necessary in order to account for the formation of  $N_2O$  and  $H_2C=O$ ; these could also be formed by a mechanism such as that given in Scheme II.

Autoacceleratory behavior could occur through bimolecular followup reactions involving attack on hydrogen and oxygen by  $H_1$  and other radical species<sup>4,9,12,15</sup> formed in the reaction, as shown in Schemes III and IV.



SCHEME I

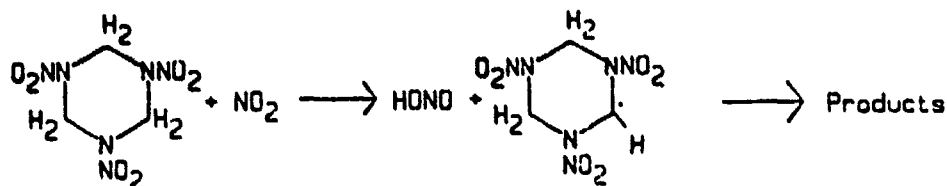


SCHEME II

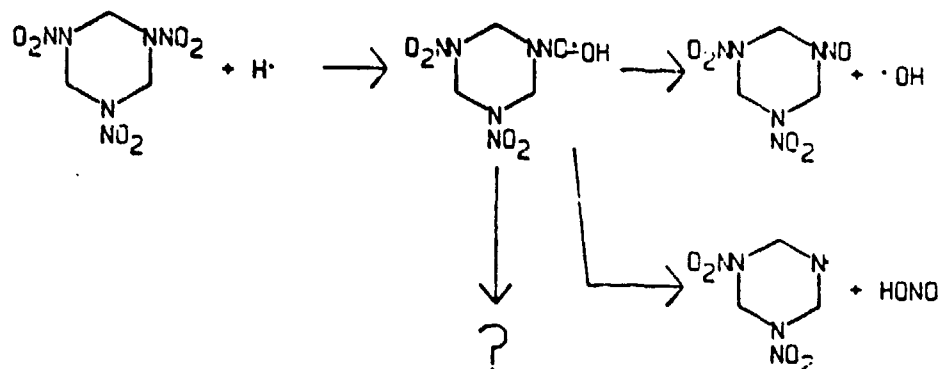


Note however that Melius and Binkley have recently argued,<sup>15</sup> on the basis of RAC-MP4 MO calculations, that the formaldehyde and N<sub>2</sub>O are not formed by the mechanisms of either Scheme I or Scheme II. They are uncertain as to the exact pathways by which these materials are formed. However their reaction schemes do include formation of NO<sub>2</sub> and H<sub>2</sub>CN. via decomposition of 3H<sub>2</sub>C=N-NO<sub>2</sub>) as shown in Scheme I above.

Furthermore, Zhao, Hintsa and Le,<sup>14a</sup> have studied RDX decomposition by infrared multiphoton dissociation and have reported that concerted pathways<sup>4</sup> (e.g., RDX → 3H<sub>2</sub>C=N-NO<sub>2</sub>) are more important than has been heretofore suspected.

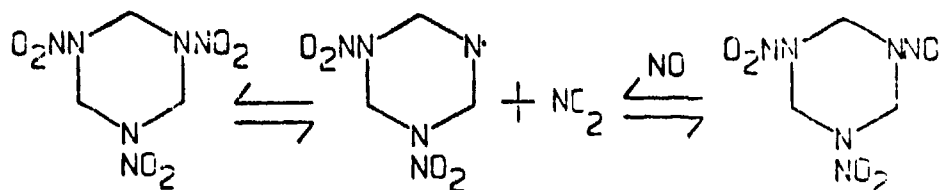


SCHEME III



SCHEME IV

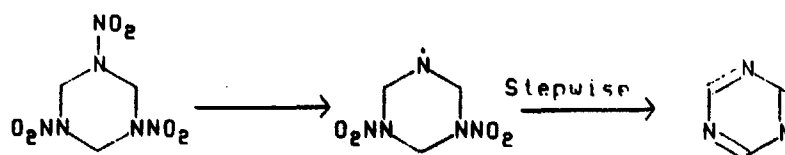
In addition to the pathway of Scheme IV, nitrosoamines could be formed via N-NO<sub>2</sub> cleavage and recombination with NO formed in the decomposition (Scheme V).



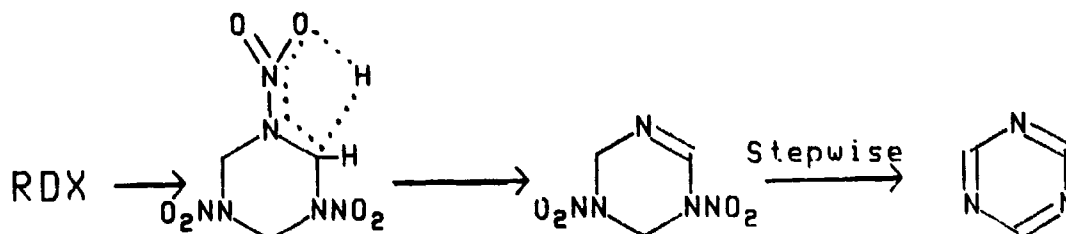
SCHEME V

The identification in the present work of 1,3,5-triazine seems of considerable interest because of its potential mechanistic significance. This significance arises because its presence indicates the occurrence of pathways not involving initial C-N cleavage; however these pathways could involve initial N-NO<sub>2</sub> cleavage, HONO elimination or H-abstraction by NO<sub>2</sub> or other radical species formed in the decomposition.

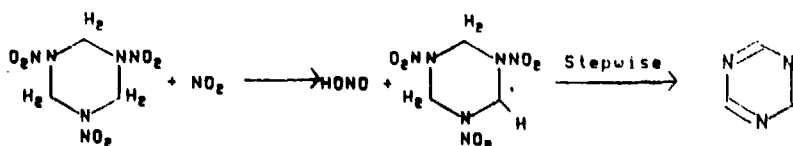
Possible mechanisms for formation of 1,3,5-triazine include: (a) formation via primary N-NO<sub>2</sub> cleavage (Scheme VI); (b) formation via primary HONO elimination (Scheme VII); (c) formation via initial abstraction of a hydrogen atom by NO<sub>2</sub> or some other radical species formed in the reaction (Scheme VIII); (d) formation via the nitroxide reported on the basis of ESR studies<sup>16</sup> (Scheme IX); and (e) trimerization of HCN formed in the decomposition of RDX (Scheme X).



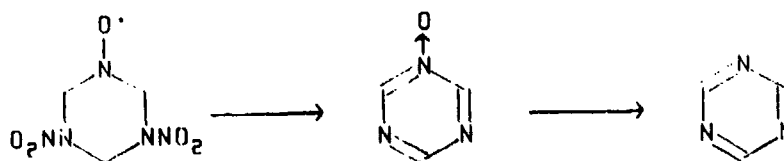
SCHEME VI



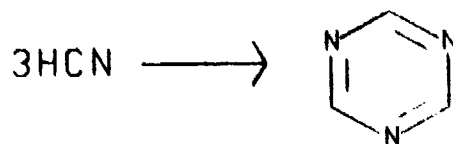
SCHEME VII



SCHEME VIII



SCHEME IX



SCHEME X

Formation of triazine via trimerization of HCN should be considered but seems relatively unlikely, since trimerization of nitriles closely related to HCN, such as  $\text{CH}_3\text{CN}$ , appears to require<sup>17</sup> not only elevated temperatures but pressures in the range 8-10 kilobars and reaction times of hours (as opposed to 20 seconds in the present work).<sup>17</sup> HCN itself trimerizes under milder conditions, but acid catalysis is apparently required.<sup>17</sup> Note that some acid products such as HONO and  $\text{HNO}_3$  can be formed in HMX and RDX decomposition.

However, it seems difficult to rule out HCN trimerization conclusively except by scrambling studies in mixtures of fully-ring-labeled and unlabeled RDX; we are presently planning to carry out such studies in connection with planned studies on N- $\text{NO}_2$  scrambling in decomposition of mixtures of fully-labeled and unlabeled RDX, both alone and in mixtures with borohydride salts. It is true that decomposition<sup>18</sup> of HMX (which does not possess a six-membered ring, but is known<sup>4,6</sup> to give HCN as a product of thermal decomposition) also gives 1,3,5-triazine. However, HMX would give 1,3,5,7-tetrazocine after loss of the elements of four molecules of HONO by pathways analogous to Schemes VI-VIII. By analogy with the known chemistry<sup>19</sup> of cyclooctatetraene, azocine and di- and triazocines (which are known<sup>19</sup> to yield respectively benzene and azabenzenes on thermolysis), it does not seem unreasonable to suppose that 1,3,5,7-tetrazocine might decompose further to 1,3,5-triazine.

The H-, HONO- and  $\text{NO}_2$ -stripping pathways shown in Schemes VI-VIII are presumably relatively minor pathways relative to the fragmentation pathways shown in Schemes I-IV. This follows from the small amounts (ca 5-10 percent) of 1,3,5-triazine (m/e 54 and 81) formed relative to m/e 44 (probably mainly  $\text{N}_2\text{O}$  and  $\text{CO}_2$ ).

Possible Chemical Mechanisms Involved in Catalysis of HMX and RDX Decomposition by Borohydride Salts. It is possible to imagine at least three main types of initial pathways which might contribute to catalysis of HMX or RDX decomposition by borohydrides:

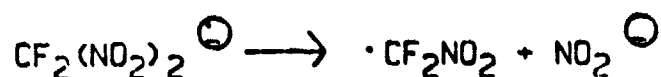
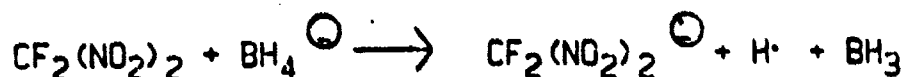
1. Decomposition of nitramine is initiated by direct reaction between nitramine and borohydride; for example by electron transfer, by attack of a B-H bond on nitro oxygen of the nitramine, or by a combination of these mechanisms.

2. An early decomposition product, for example  $\text{NO}_2$ , of the nitramine reacts with the catalyst to form products or intermediates, possibly free radicals, which react further with the nitramine, resulting in catalysis.

3. Unimolecular decomposition of the catalyst generates products or intermediates which react with nitramine, causing it to decompose faster than it otherwise would.

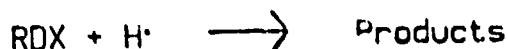
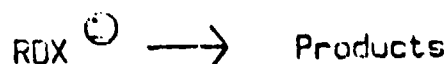
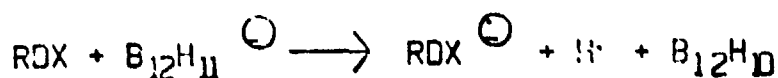
At present there is insufficient evidence to distinguish between these possibilities. Nevertheless, the following comments seem relevant.

A possible pathway of type (1) can be written based on a suggestion<sup>20</sup> contained in a Russian study of the reaction of a variety of nucleophilic reagents, including sodium borohydride ( $\text{NaBH}_4$ ), with difluorodinitromethane,  $\text{CF}_2(\text{NO}_2)_2$ . The radicals produced were studied by ESR and trapping techniques, and identified as  $\text{H}\cdot$  and  $\cdot\text{CF}_2\text{NO}_2$ . Their formation was rationalized in terms of the following mechanism:



#### SCHEME XI

An analogous mechanism for catalysis of RDX decomposition by  $\text{K}_2\text{B}_{12}\text{H}_{12}$  or  $\text{K}_2\text{B}_{10}\text{H}_{10}$  might be written as follows:



#### SCHEME XII

Pathway (3) seems relatively unlikely, at least at lower temperatures; this is based on the apparent inertness<sup>21</sup> of salts closely related to  $\text{K}_2\text{B}_{12}\text{H}_{12}$  when treated under conditions (200–500°C) as severe or more so than the 200–300°C temperatures which cause decomposition of HMX or RDX alone, and at which borohydride catalysis of HMX/RDX decomposition is observed. However it was reported<sup>21</sup> that above 505°C,  $\text{Na}_2\text{B}_{12}\text{H}_{12}$  underwent exothermic thermal-oxidative degradation accompanied by a gain in weight equivalent to one oxygen atom per formula weight of the anhydrous salt, and that above 830°C it burned.

#### ACKNOWLEDGEMENTS

The author thanks Robert A. Fifer for many helpful discussions and for reading and commenting extensively on a preliminary draft of this manuscript, and Indu B. Mishra for reading and commenting extensively on a preliminary draft of this manuscript and for calling our attention to the possible presence of boron-fragment peaks in some of the mass spectra.

## REFERENCES

1. M.A. Schroeder, "Critical Analysis of Nitramine Decomposition Data: Some Suggestions for Needed Research Work," BRL Memorandum Report ARBRL-MR-3181, June 1982, AD-A116 194.
2. M.A. Schroeder, "Critical Analysis of Nitramine Decomposition Data: Preliminary Comments on Autoacceleration and Autoinhibition in HMX and RDX Decomposition in HMX and RDX Decomposition," Memorandum Report ARBRL-MR-03370, August 1984, AD-A146 570.
3. M.A. Schroeder, "Critical Analysis of Nitramine Decomposition Data: Activation Energies and Frequency Factors for HMX and RDX Decomposition," Technical Report BRL-TR-2673, September 1985, AD-A160 543.
4. M.A. Schroeder, "Critical Analysis of Nitramine Decomposition Data: Product Distributions from HMX and RDX Decomposition," Technical Report BRL-TR-2659, June 1985, AD-A159 325.
5. M.A. Schroeder, "Critical Analysis of Nitramine Decomposition Results: Some Comments on Chemical Mechanisms," Proceedings of 16th JANNAF Combustion Meeting, CPIA Publication No. 308, Vol. II, pp. 17-34, September 1979.
6. M.A. Schroeder, "Critical Analysis of Nitramine Decomposition Data: Update, Some Comments on Pressure and Temperature Effects and Wrap-Up Discussion of Chemical Mechanisms," Proceedings of 21st JANNAF Combustion Meeting, CPIA Publication 412, Vol. II, pp. 595-614, October 1984.
7. R.A. Fifer, "Chemistry of Nitrate Ester and Nitramine Propellants," in "Fundamentals of Solid Propellant Combustion," K.K. Kuo and M. Summerfield, Eds., Vol. 90 of Progress in Astronautics and Aeronautics Series, AIAA, New York, 1984.
8. J.C. Hoffsommer and D.J. Glover, "Thermal Decomposition of 1,3,5-Triazacyclohexane (RDX): Kinetics of Nitroso Intermediates Formation," Combustion and Flame, Vol. 59, pp. 303-310, 1985.
9. R.A. Fifer, S.A. Liebman, P.J. Duff, K.D. Fickie and M.A. Schroeder, "Thermal Degradation Mechanisms of Nitramine Propellants," Proceedings of 22nd JANNAF Combustion Meeting, CPIA Publication 432, Vol. II, pp. 537-546, October 1985.
10. J.C. Hoffsommer, D.J. Glover, and W.L. Elban, "Quantitative Evidence for Nitroso Compound Formation in Drop-Weight Impacted RDX Crystals," Journal of Energetic Materials, Vol. 3, pp. 149-167, 1985.
11. P. Snyder, J. Kremer, and S.A. Liebman, CRDEC, Aberdeen Proving Ground, Maryland, private communication, September 1986.
12. J.N. Bradley, A.K. Butler, W.D. Capey, and J. R. Gilbert, "Mass Spectrometric Study of the Thermal Decomposition of 1,3,5-Trinitrohexahydro-1,3,5-triazine (RDX)," J. Chem. Soc., Faraday Trans., Part 1, Vol. 73, pp. 1789-95, 1977.

13. B.B. Goshgarian, "The Thermal Decomposition of Cyclotrimethylene-trinitramine (RDX) and Cyclotetramethylenetetranitramine (HMX)," AFRPL-TR-78-76, October 1978, AD-B032 275L.
- 14a. X. Zhao, E.J. Hintsa, and Y. T. Lee, "Infrared Multiphoton Dissociation of RDX in a Molecular Beam," Report ONR NR 659-819/7/87, 7 July 1987, submitted to Journal of Chemical Physics.
- b. J.F. Ditter, F.J. Gerhart, and R.E. Williams, "Analysis of Boranes and Carboranes by Mass Spectrometry," in Mass Spectrometry in Inorganic Chemistry, Advances in Chemistry Series, No. 72, American Chemical Society, Washington, DC, p. 191, 1968.
15. C.F. Melius and J.S. Binkley, "Thermochemistry of the Decomposition of Nitramines in the Gas Phase," accepted for publication in the Proceedings of the 21st International Combustion Symposium.
- 16a. M.D. Pace, "Thermal Decomposition of RDX: Evidence of a Nitronylnitroxyl Free Radical Intermediate," Journal of Energetic Materials, Vol. 3, pp. 279-291, 1985.
- b. M.D. Pace, A.D. Britt, W.B. Moniz, and D. Stec, III, "Paramagnetic Decomposition Products from Energetic Materials", Preprints of papers to be presented at the Eighth Symposium (International) on Detonation, Albuquerque, Volume I, pp. 441-448, 15-19 July 1985.
17. D. Martin, M. Bauer, and V. A. Pankratov, "Cyclization of Cyano-Compounds into 1,3,5-Triazines," Uspekhi Khimii, Vol. 47, p. 1814, 1978; Russian Chemical Reviews, Vol. 47, pp. 975-990, 1978.
18. M.A. Schroeder, Unpublished work, 1987.
- 19a. S. Yogi, K. Hokama, and O. Tsuge, "A Stable 1,2-Diazocine System: 3,8-Diphenyl-1,2-Diazacycloocta-2,4,6,8-Tetraenes," Chemistry Letters, pp. 1579-1582, 1982.
- b. B.M. Trost, P.H. Scudder, R.M. Cory, N.J. Turro, V. Ramanurthy, and T.J. Katz, "1,2-Diaza-2,4,6,8-cyclooctatetraene," J. Org. Chem., Vol. 44, pp. 1264-1269, 1979.
- c. D. Dudek, K. Glanzer and J. Troe, "Pyrolysis of 1,3,5,7-Cyclooctatetraene, Semibullvalene and 1,5-Dihydropentalene in Shock Waves and in a Flow System (Part I)," Ber. Bunsenges. Phys. Chem., Vol. 83, pp. 776-788, 1979.
20. L.V. Okhlobystina, T.I. Cherkasova, and V.A. Tyurikov, "Study of the Formation of Free Radicals in Reactions of Aliphatic Nitro Compounds by the Method of Radical Trapping. 4. Formation of Short-Lived Radicals When Nucleophilic Reagents are Reacted with Difluorodinitromethane in Aprotic Solvents," Izv. Akad. Nauk SSSR, Ser. Khim., pp. 2214-2220, 1979, English Translation, pp. 2036-2043.
21. K.A. Solntsev, N.T. Kuznetsov, and V.I. Ponomarev, "Physical Properties and Structural Characteristics of Closo-Dodecaborate Tetrahydrate," Dokl. Akad. Nauk. SSSR, Vol. 228, pp. 853-856, 1976; English Translation, pp. 391-394.

# DISTRIBUTION LIST

<u>No. Of Copies</u>	<u>Organization</u>	<u>No. Of Copies</u>	<u>Organization</u>
12	Administrator Defense Technical Info Center ATTN: DTIC-FDAC Cameron Station, Bldg. 5 Alexandria, VA 22304-6145	1	Director US Army Aviation Research and Technology Activity Ames Research Center Moffett Field, CA 94035-1099
1	HQ DA DAMA-ART-M Washington, DC 20310	4	Commander US Army Research Office ATTN: R. Ghirardelli D. Mann R. Singleton R. Shaw P.O. Box 12211 Research Triangle Park, NC 27709-2211
1	Commander US Army Materiel Command ATTN: AMCDRA-ST 5001 Eisenhower Avenue Alexandria, VA 22333-0001		
10	C.I.A. OIR/DB/Standard GE47 HQ Washington, DC 20505	1	Commander US Army Communications - Electronics Command ATTN: AMSEL-ED Fort Monmouth, NJ 07703
1	Commander US Army ARDEC ATTN: SMCAR-MSI Dover, NJ 07801-5001	1	Commander CECOM R&D Technical Library ATTN: AMSEL-IM-L, Reports Section B.2700 Fort Monmouth, NJ 07703-5000
1	Commander US Army ARDEC ATTN: SMCAR-TDC Dover, NJ 07801	2	Commander Armament R&D Center US Army AMCCOM ATTN: SMCAR-LCA-G, D.S. Downs J.A. Lannon Dover, NJ 07801
1	Commander US AMCCOM ARDEC CCAC Benet Weapons Laboratory ATTN: SMCAR-CCB-TL Watervliet, NY 12189-4050		
1	US Army Armament, Munitions and Chemical Command ATTN: AMSMC-IMP-L Rock Island, IL 61299-7300	1	Commander Armament R&D Center US Army AMCCOM ATTN: SMCAR-LC-G, L. Harris Dover, NJ 07801
1	Commander US Army Aviation Systems Command ATTN: AMSAV-ES 4300 Goodfellow Blvd. St. Louis, MO 63120-1798	1	Commander Armament R&D Center US Army AMCCOM ATTN: SMCAR-SCA-T, L. Stiefel Dover, NJ 07801



# DISTRIBUTION LIST

<u>No. Of Copies</u>	<u>Organization</u>	<u>No. Of Copies</u>	<u>Organization</u>
1	Commander US Army Missile Command Research, Development and Engineering Center ATTN: AMSMI-RD Redstone Arsenal, AL 35898	1	Office of Naval Research Department of the Navy ATTN: R.S. Miller, Code 432 800 N. Quincy Street Arlington, VA 22217
1	Commander US Army Missile and Space Intelligence Center ATTN: AMSMI-YDL Redstone Arsenal, AL 35898-5000	1	Commander Naval Air Systems Command ATTN: J. Ramnarace, AIR-54111C Washington, DC 20360
2	Commander US Army Missile Command ATTN: AMSMI-RK, D.J. Ifshin W. Wharton Redstone Arsenal, AL 35898	2	Commander Naval Ordnance Station ATTN: C. Irish P.L. Stang, Code 515 Indian Head, MD 20640
1	Commander US Army Missile Command ATTN: AMSMI-RKA, A.R. Maykut Redstone Arsenal, AL 35898-5249	1	Commander Naval Surface Weapons Center ATTN: J.L. East, Jr., G-23 Dahlgren, VA 22448-5000
1	Commander US Army Tank Automotive Command ATTN: AMSTA-TSL Warren, MI 48397-5000	2	Commander Naval Surface Weapons Center ATTN: R. Bernecker, R-13 G.B. Wilmot, R-16 Silver Spring, MD 20902-5000
1	Director US Army TRADOC Systems Analysis Center ATTN: ATOR-TSL White Sands Missile Range, NM 88002-5502	1	Commander Naval Weapons Center ATTN: R.L. Derr, Code 389 China Lake, CA 93555
1	Commandant US Army Infantry School ATTN: ATSH-CD-CS-OR Fort Benning, GA 31905-5400	2	Commander Naval Weapons Center ATTN: Code 3891, T. Boggs K.J. Graham China Lake, CA 93555
1	Commander US Army Development and Employment Agency ATTN: MODE-ORO Fort Lewis, WA 98433-5000	5	Commander Naval Research Laboratory ATTN: M.C. Lin J. McDonald E. Oran J. Shnur R.J. Doyle, Code 6110 Washington, DC 20375

# DISTRIBUTION LIST

<u>No. Of Copies</u>	<u>Organization</u>	<u>No. Of Copies</u>	<u>Organization</u>
1	Commanding Officer Naval Underwater Systems Center Weapons Dept. ATTN: R.S. Lazar/Code 36301 Newport, RI 02840	1	OSD/SDIO/UST ATTN: L.H. Caveny Pentagon Washington, DC 20301-7100
1	Superintendent Naval Postgraduate School Dept. of Aeronautics ATTN: D.W. Netzer Monterey, CA 93940	1	Aerojet Solid Propulsion Co. ATTN: P. Micheli Sacramento, CA 95813
4	AFRPL/DY, Stop 24 ATTN: R. Corley R. Geisler J. Levine D. Weaver Edwards AFB, CA 93523-5000	1	Applied Combustion Technology, Inc. ATTN: A.M. Varney P.O. Box 17885 Orlando, FL 32860
1	AFRPL/MKPB, Stop 24 ATTN: B. Goshgarian Edwards AFB, CA 93523-5000	2	Applied Mechanics Reviews The American Society of Mechanical Engineers ATTN: R.E. White A.B. Wenzel 345 E. 47th Street New York, NY 10017
1	AFOSR ATTN: J.M. Tishkoff Bolling Air Force Base Washington, DC 20332	1	Atlantic Research Corp. ATTN: M.K. King 5390 Cherokee Avenue Alexandria, VA 22314
1	AFATL/DOIL (Tech Info Center) Eglin AFB, FL 32542-5438	1	Atlantic Research Corp. ATTN: R.H.W. Waesche 7511 Wellington Road Gainesville, VA 22065
1	Air Force Weapons Laboratory AFWL/SUL ATTN: V. King Kirtland AFB, NM 87117	1	AVCO Everett Rsch. Lab. Div. ATTN: D. Stickler 2385 Revere Beach Parkway Everett, MA 02149
1	NASA Langley Research Center Langley Station ATTN: G.B. Northam/MS 168 Hampton, VA 23365	1	Battelle Memorial Institute Tactical Technology Center ATTN: J. Huggins 505 King Avenue Columbus, OH 43201
4	National Bureau of Standards ATTN: J. Hastie M. Jacox T. Kashiwagi H. Semerjian US Department of Commerce Washington, DC 20234	1	Cohen Professional Services ATTN: N.S. Cohen 141 Channing Street Redlands, CA 92373

# DISTRIBUTION LIST

<u>No. Of Copies</u>	<u>Organization</u>	<u>No. Of Copies</u>	<u>Organization</u>
1	Exxon Research & Eng. Co. ATTN: A. Dean Route 22E Annandale, NJ 08801	1	Hercules, Inc. Bacchus Works ATTN: K.P. McCarty P.O. Box 98 Magna, UT 84044
1	Ford Aerospace and Communications Corp. DIVAD Division Div. Hq., Irvine ATTN: D. Williams Main Street & Ford Road Newport Beach, CA 92663	1	Honeywell, Inc. Government and Aerospace Products ATTN: D.E. Broden/ MS MN50-2000 600 2nd Street NE Hopkins, MN 55343
1	General Applied Science Laboratories, Inc. ATTN: J.I. Erdos 425 Merrick Avenue Westbury, NY 11590	1	IBM Corporation ATTN: A.C. Tam Research Division 5600 Cottle Road San Jose, CA 95193
1	General Electric Armament & Electrical Systems ATTN: M.J. Bulman Lakeside Avenue Burlington, VT 05401	1	IIT Research Institute ATTN: R.F. Remaly 10 West 35th Street Chicago, IL 60616
1	General Electric Company 2352 Jade Lane Schenectady, NY 12309	2	Director Lawrence Livermore National Laboratory ATTN: C. Westbrook M. Costantino P.O. Box 808 Livermore, CA 94550
1	General Electric Ordnance Systems ATTN: J. Mandzy 100 Plastics Avenue Pittsfield, MA 01203	1	Lockheed Missiles & Space Co. ATTN: George Lo 3251 Hanover Street Dept. 52-35/B204/2 Palo Alto, CA 94304
2	General Motors Rsch Labs Physics Department ATTN: T. Sloan R. Teets Warren, MI 48090	1	Los Alamos National Lab ATTN: B. Nichols T7, MS-B284 P.O. Box 1663 Los Alamos, NM 87545
2	Hercules, Inc. Allegany Ballistics Lab. ATTN: R.R. Miller E.A. Yount P.O. Box 210 Cumberland, MD 21501	1	National Science Foundation ATTN: A.B. Harvey Washington, DC 20550

# DISTRIBUTION LIST

<u>No. Of Copies</u>	<u>Organization</u>	<u>No. Of Copies</u>	<u>Organization</u>
1	Olin Corporation Smokeless Powder Operations ATTN: V. McDonald P.O. Box 222 St. Marks, FL 32355	3	SRI International ATTN: G. Smith D. Crosley D. Golden 333 Ravenswood Avenue Menlo Park, CA 94025
1	Paul Gough Associates, Inc. ATTN: P.S. Gough 1048 South Street Portsmouth, NH 03801	1	Stevens Institute of Tech. Davidson Laboratory ATTN: R. McAlevy, III Hoboken, NJ 07030
2	Princeton Combustion Research Laboratories, Inc. ATTN: M. Summerfield N.A. Messina 475 US Highway One Monmouth Junction, NJ 08852	1	Textron, Inc. Bell Aerospace Co. Division ATTN: T.M. Ferger P.O. Box 1 Buffalo, NY 14240
1	Hughes Aircraft Company ATTN: T.E. Ward 8433 Fallbrook Avenue Canoga Park, CA 91303	1	Thiokol Corporation Elkton Division ATTN: W.N. Brundige P.O. Box 241 Elkton, MD 21921
1	Rockwell International Corp. Rocketdyne Division ATTN: J.E. Flanagan/HB02 6633 Canoga Avenue Canoga Park, CA 91304	1	Thiokol Corporation Huntsville Division ATTN: R. Glick Huntsville, AL 35807
4	Sandia National Laboratories Combustion Sciences Dept. ATTN: R. Cattolica S. Johnston P. Mattern D. Stephenson Livermore, CA 94550	3	Thiokol Corporation Wasatch Division ATTN: S.J. Bennett P.O. Box 524 Brigham City, UT 84302
1	Science Applications, Inc. ATTN: R.B. Edelman 23146 Cumorah Crest Woodland Hills, CA 91364	1	TRW ATTN: M.S. Chou MSR1-1016 1 Parke Redondo Beach, CA 90278
1	Science Applications, Inc. ATTN: H.S. Pergament 1100 State Road, Bldg. N Princeton, NJ 08540	1	United Technologies ATTN: A.C. Eckbreth East Hartford, CT 06108

# DISTRIBUTION LIST

<u>No. Of Copies</u>	<u>Organization</u>	<u>No. Of Copies</u>	<u>Organization</u>
3	United Technologies Corp. Chemical Systems Division ATTN: R.S. Brown T.D. Myers (2 copies) P.O. Box 50015 San Jose, CA 95150-0015	1	University of California Los Alamos Scientific Lab. P.O. Box 1663, Mail Stop B216 Los Alamos, NM 87545
2	United Technologies Corp. ATTN: R.S. Brown R.O. McLaren P.O. Box 358 Sunnyvale, CA 94086	2	University of California, Santa Barbara Quantum Institute ATTN: K. Schofield M. Steinberg Santa Barbara, CA 93106
1	Universal Propulsion Company ATTN: H.J. McSpadden Black Canyon Stage 1 Box 1140 Phoenix, AZ 85029	2	University of Southern California Dept. of Chemistry ATTN: S. Benson C. Wittig Los Angeles, CA 90007
1	Veritay Technology, Inc. ATTN: E.B. Fisher 4845 Millersport Highway P.O. Box 305 East Amherst, NY 14051-0305	1	Case Western Reserve Univ. Div. of Aerospace Sciences ATTN: J. Tien Cleveland, OH 44135
1	Brigham Young University Dept. of Chemical Engineering ATTN: M.W. Beckstead Provo, UT 84601	1	Cornell University Department of Chemistry ATTN: T.A. Cool Baker Laboratory Ithaca, NY 14853
1	California Institute of Tech. Jet Propulsion Laboratory ATTN: MS 125/159 4800 Oak Grove Drive Pasadena, CA 91103	1	Univ. of Dayton Rsch Inst. ATTN: D. Campbell AFRPL/PAP Stop 24 Edwards AFB, CA 93523
1	California Institute of Technology ATTN: F.E.C. Culick/ MC 301-46 204 Karman Lab. Pasadena, CA 91125	1	University of Florida Dept. of Chemistry ATTN: J. Winefordner Gainesville, FL 32611
1	University of California, Berkeley Mechanical Engineering Dept. ATTN: J. Daily Berkeley, CA 94720	3	Georgia Institute of Technology School of Aerospace Engineering ATTN: E. Price W.C. Strahle B.T. Zinn Atlanta, GA 30332

# DISTRIBUTION LIST

<u>No. Of Copies</u>	<u>Organization</u>	<u>No. Of Copies</u>	<u>Organization</u>
1	University of Illinois Dept. of Mech. Eng. ATTN: H. Krier 144MEB, 1206 W. Green St. Urbana, IL 61801	1	Princeton University MAE Dept. ATTN: F.A. Williams Princeton, NJ 08544
1	Johns Hopkins University/APL Chemical Propulsion Information Agency ATTN: T.W. Christian Johns Hopkins Road Laurel, MD 20707	1	Purdue University School of Aeronautics and Astronautics ATTN: J.R. Osborn Grissom Hall West Lafayette, IN 47906
1	University of Michigan Gas Dynamics Lab Aerospace Engineering Bldg. ATTN: G.M. Faeth Ann Arbor, MI 48109-2140	1	Purdue University Department of Chemistry ATTN: E. Grant West Lafayette, IN 47906
1	University of Minnesota Dept. of Mechanical Engineering ATTN: E. Fletcher Minneapolis, MN 55455	2	Purdue University School of Mechanical Engineering ATTN: N.M. Laurendeau S.N.B. Murthy TSPC Chaffee Hall West Lafayette, IN 47906
3	Pennsylvania State University Applied Research Laboratory ATTN: K.K. Kuo H. Palmer M. Micci University Park, PA 16802	1	Rensselaer Polytechnic Inst. Dept. of Chemical Engineering ATTN: A. Fontijn Troy, NY 12181
1	Pennsylvania State University Dept. of Mechanical Engineering ATTN: V. Yang University Park, PA 16802	1	Stanford University Dept. of Mechanical Engineering ATTN: R. Hanson Stanford, CA 94305
1	Polytechnic Institute of NY Graduate Center ATTN: S. Lederman Route 110 Farmingdale, NY 11735	1	University of Texas Dept. of Chemistry ATTN: W. Gardiner Austin, TX 78712
2	Princeton University Forrestal Campus Library ATTN: K. Brezinsky I. Glassman P.O. Box 710 Princeton, NJ 08540	1	University of Utah Dept. of Chemical Engineering ATTN: G. Flandro Salt Lake City, UT 84112

## DISTRIBUTION LIST

No. Of  
Copies

Organization

1	Virginia Polytechnic Institute and State University ATTN: J.A. Schetz Blacksburg, VA 24061
1	Commandant USAFAS ATTN: ATSF-TSM-CN Fort Sill, OK 73503-5600
1	F.J. Seiler Research Lab (AFSC) ATTN: S.A. Shakelford USAF Academy, CO 80840-6528

Aberdeen Proving Ground

Dir, USAMSAA  
ATTN: AMXSY-D  
AMXSY-MP, H. Cohen  
Cdr, USATECOM  
ATTN: AMSTE-SI-F  
Cdr, CRDC, AMCCOM  
ATTN: SMCCR-RSP-A  
SMCCR-MU  
SMCCR-SPS-IL

### USER EVALUATION SHEET/CHANGE OF ADDRESS

This Laboratory undertakes a continuing effort to improve the quality of the reports it publishes. Your comments/answers to the items/questions below will aid us in our efforts.

1. BRL Report Number \_\_\_\_\_ Date of Report \_\_\_\_\_

2. Date Report Received \_\_\_\_\_

3. Does this report satisfy a need? (Comment on purpose, related project, or other area of interest for which the report will be used.) \_\_\_\_\_  
\_\_\_\_\_  
\_\_\_\_\_

4. How specifically, is the report being used? (Information source, design data, procedure, source of ideas, etc.) \_\_\_\_\_  
\_\_\_\_\_  
\_\_\_\_\_

5. Has the information in this report led to any quantitative savings as far as man-hours or dollars saved, operating costs avoided or efficiencies achieved, etc? If so, please elaborate. \_\_\_\_\_  
\_\_\_\_\_  
\_\_\_\_\_

6. General Comments. What do you think should be changed to improve future reports? (Indicate changes to organization, technical content, format, etc.) \_\_\_\_\_  
\_\_\_\_\_  
\_\_\_\_\_  
\_\_\_\_\_

CURRENT  
ADDRESS

\_\_\_\_\_  
Name

\_\_\_\_\_  
Organization

\_\_\_\_\_  
Address

\_\_\_\_\_  
City, State, Zip

7. If indicating a Change of Address or Address Correction, please provide the New or Corrected Address in Block 6 above and the Old or Incorrect address below.

OLD  
ADDRESS

\_\_\_\_\_  
Name

\_\_\_\_\_  
Organization

\_\_\_\_\_  
Address

\_\_\_\_\_  
City, State, Zip

(Remove this sheet, fold as indicated, staple or tape closed, and mail.)



----- FOLD HERE -----

Director  
U.S. Army Ballistic Research Laboratory  
ATTN: SLCHR-DD-T  
Aberdeen Proving Ground, MD 21005-5066



NO POSTAGE  
NECESSARY  
IF MAILED  
IN THE  
UNITED STATES

OFFICIAL BUSINESS  
PENALTY FOR PRIVATE USE, \$300

**BUSINESS REPLY MAIL**  
FIRST CLASS PERMIT NO 12062 WASHINGTON, DC  
POSTAGE WILL BE PAID BY DEPARTMENT OF THE ARMY

Director  
U.S. Army Ballistic Research Laboratory  
ATTN: SLCHR-DD-T  
Aberdeen Proving Ground, MD 21005-9989

----- FOLD HERE -----